Iowa State Water Resources Research Institute

Annual Technical Report

FY 2000

Introduction

ISWRRI is a multi-campus institute that has conducted research, educational and outreach programs on Iowa's water related problems for the past 36 years. ISWRRI's mission is to develop statewide linkages between universities and public and private sectors and promote education, research and information transfer on water resources and water quality issues in Iowa. ISWRRI is important to Iowa because its work focuses on protecting Iowa's waters, a resource that makes Iowa a leader in agricultural production.

Protecting Iowa's natural resources has been a major challenge for Iowa's policy makers. Several positive things have happened in the recent past. Last year, Iowa's legislature and the governor took major steps in developing a new $11.2 million Water Quality Initiative to develop programs to protect Iowa's water resources. This initiative provides ISWRRI an excellent opportunity to work with state agencies in developing joint projects and interdisciplinary teams to solve current and emerging water quality problems in Iowa. Iowa's three regent universities and other educational institutions have outstanding faculty and staff working in the water science area.

The Water Resources Act of 1984 requires that ISWRRI be evaluated periodically to determine its eligibility for continued support of federal funds. In November 1999, ISWRRI was placed on probation and faced the threat of losing federal funds. I was appointed ISWRRI's new director in December 1999 and my major challenge was to regain federal funding within one year. ISWRRI's newly appointed faculty advisory committee and state advisory research panel provided exemplary leadership, energy and time in developing ISWRRI's new five-year (2001-2005) strategic plan. The dean of ISU's College of Agriculture, who also is the director of the Iowa Agricultural Experiment Station and the vice provost of research made a three year commitment to provide additional funds to strengthen ISWRRI's competitive research grants program. The additional funding and visionary guidance of ISWRRI's faculty advisory council and support from the Iowa Departments of Natural Resources and Agriculture and Land Stewardship allowed the development of several new programs in 2000. In March 2001, ISWRRI won back its standing and was removed from probationary status.

Research Program

Basic Information

Title:	A prediction system for transport and fate of toxic substances in surface waters
Project Number:	B-03
Start Date:	3/1/1999
End Date:	2/28/2001
Research Category:	Not Applicable
Focus Category:	Toxic Substances, Models, Water Quality
Descriptors:	Water quality modeling, toxic substances, contaminant transport, rivers, reservoirs, water quality control
Lead Institute:	Iowa State Water Resources Research Institute
Principal Investigators:	Ruochuan Gu

Publication

1. Tang, L. 2001. Development and applications of a reservoir water quality prediction system. M.S. Thesis, Iowa State University. 2001.

Problems and research objectives:

Toxic substances from chemical spills and non-point source runoff into rivers, reservoirs or lakes pose a potential risk to human health and aquatic lives. Accidental spills can be caused by train derails and truck collisions during ground transportation, leaking from factories and storage tanks, and obsolete navigation (barges in the Midwest waterways and tankers in other regions). Toxic contaminants from spills and runoff have a significant impact on the environment and continue to be a serious threat to the Nation's and regional watersheds and water resources. The inevitability of toxic spills and runoff points to the need for a full understanding of the behavior (transport and fate) of toxic chemicals in surface waters and an effective tool for prediction to assist contamination control, remediation management and watershed protection. On the other hand, lack of understanding of toxic substance behavior in a reservoir can hamper effective implementation of spill control measures.

The **objectives** of the research are (1) to develop and validate an integrated 2-D mathematical model that simulates and predicts the fate and transport of toxic chemical spills and runoff in rivers and reservoirs or lakes, (2) to develop a real-time prediction and analysis computer program for emergency responses and remediation management, and (3) to incorporate the prediction system into an existing regional contingency plan or a toxic contamination control program at the state level.

Methodology

This research project will develop and validate an integrated 2-D mathematical model and a real-time computer program that predicts the fate and transport of toxic substances in rivers and reservoirs or lakes, investigates the flow behavior and mixing processes in various flow regimes, and evaluates their effects on the dilution of spilled or runoff-carried chemicals and water quality conditions in a stratified reservoir or lake.

The three components and interactions of toxic substances in a stream and reservoir system (flow of water, transport of sediments, and fate and transport of toxic chemicals) will be formulated and integrated. The physical and biochemical processes will be internally linked by coupling the unsteady equations for flows, sediments, and toxic contaminants.

The model simulating the fate and transport of spilled or non-point source toxic chemicals will be incorporated into a computer prediction and analysis program consisting of the following three modules for ease and quickness: (1) a menu-based pre-processor for interactive data preparation and execution of other modules, (2) the spill model for prediction, simulation, and analysis, and (3) a post-processor that provides a graphic interface for visualizing the results of the spill model to keep track of a spill in a waterbody.

The model to be developed will be tested and validated against the field data of past spills into the Sacramento River and Shasta Reservoir and the observations of contaminated density currents (carrying toxic chemicals) in Des Moines River and Saylorville Reservoir, Iowa. This test will focus on the fate and transport of pesticides, including atrazine, alachlor, and dieldrin.

Findings

A menu-driven reservoir Water Quality Prediction System (WQPS) has been developed in this study. It is user-friendly and computationally efficient. It runs within and fully supports

the Microsoft Windows environment. It uses the latest graphical user interface (GUI) technology for interactive data entry, menu-driven model execution, and graphical visualization and display of program results. All TOXI-W2 program features and options have been implemented in WQPS. Users can interact with WQPS through the GUI. The prediction system has been tested by applications to the Saylorville Reservoir. Its practical usefulness has been demonstrated through two case studies.

Applications of WQPS have been made to the simulations of atrazine fate and transport and temperature profiles in the Saylorville Reservoir. A comparison of the simulation results for atrazine and field measurements indicated a reasonable good agreement and some overestimations.

Non-point source loading and atrazine half-life are very important to the simulations of atrazine concentrations in the reservoir. Case studies have been conducted to analyze the sensitivity of atrazine to half-life and application rate. It is concluded that atrazine concentration is linearly related to the application rate, which determines the non-point source loading rate. Atrazine concentration increases linearly with the non-point source loading rate. The results of the sensitivity analysis showed the significance of non-point source contributions to the atrazine concentrations in the Saylorville Reservoir.

Atrazine concentration increases with the half-life. Results from the case study of atrazine response to half-life indicated that the sensitivity of concentration to half-life is much greater at short half-life than at long ones. It is concluded that atrazine in a reservoir is not sensitive to half-life longer than 150 days.

It is recommended that the improvements could be made in the contour of WQPS to the level of some popular contour software such as SURFER. The future work suggested for the user interface is to add the flow field to the graph option. A more sophisticated turbulence model may be used for more detailed and accurate simulations of the flow fields. Other variables such as the partition coefficient in water and bed sediment also need further studies.

The Water Quality Prediction System can provide information on the locations in a receiving waterbody and concentrations of toxic or conventional chemicals carried by a discharge, a spill or a runoff. It serves as a tool for quick analysis/assessment, emergency response for contamination control, and reservoir management within a short period after an actual incident. Predicting the location and concentration of toxic pollutants can guide data collection during a discharge, spill or runoff event. The program can be used to make predictions, to warn water plants about closing intake structures, and to notify fisheries and reservoir management personnel to minimize the concentration consequences of toxic pollutant discharges, runoff or spills.

Basic Information

Title:	Field assessment of groundwater quality beneath cracking soil with surface-applied hog manure
Project Number:	B-04
Start Date:	3/1/1999
End Date:	2/28/2001
Research Category:	Not Applicable
Focus Category:	Agriculture, Groundwater, Non Point Pollution
Descriptors:	Agriculture, animal waste, contaminant transport, groundwater quality, hydrology, infiltration, mathematical models, soil physics, surface-groundwater relationships, unsaturated flow, water quality modeling
Lead Institute:	Iowa State Water Resources Research Institute
Principal Investigators:	Robert Horton

Publication

1. Tabbara, H., J.H. Lee, and R. Horton. 2000. Swine manure transport in soils using time domain reflectometry. p 210. Agronomy Abstract, 2000 Annual Meetings. Madison, WI. Nov. 5-9, 2000.
2. Lee, J.H., R. Horton, and H. Tabbara. Transport of swine manure in soil cores. Trans. ASAE. (In preparation)
3. Ella, V.B., J.H. Lee, R. Horton. Measurements of swine manure transport in soil using TDR: A Lysimeter study. Trans. ASAE. (In preparation)

Introduction

The threat to groundwater contamination by swine manure continues to be a major concern particularly in Iowa, where numerous large hog confinement facilities exist. While a number of studies have been done on groundwater quality effects of livestock manure application and on methods to reduce manure impact on both surface and groundwater resources, studies on the preferential flow of manure have received very little attention. In order to develop appropriate swine manure application strategies that will reduce groundwater quality degradation, detailed studies of preferential transport in various situations need to be conducted.

From the instrumentation standpoint, this research project is believed to be a pioneering work as no study on swine manure transport in soils using TDR has ever been reported in published literature. Although this relatively new method for gathering water content and bulk EC data has shown applicability in a number of solute transport experiments, no attempt on using this method for monitoring swine manure transport has been documented. Hence, research efforts geared towards the use of TDR for monitoring manure transport in soils could be considered to be an important research strategy towards fulfilling the overall goal of investigating and characterizing manure impacts on groundwater quality, particularly for preferential flow in Iowa.

The main objectives of this research were:

1. To develop and test a method for measuring preferential water and manure transport using TDR and undisturbed soil cores; A laboratory study
2. To obtain field-measured data on preferential water and manure transfer using TDR; A lysimeter study

Materials and Methods

Theory

A simple and rapid field applicable procedure for determining solute transport properties based on TDR measurements was proposed by Kachanoski et al. (1992) and tested by Elrick et al. (1992). This method uses vertically installed TDR probes with a very short pulse of tracer application. The TDR measurements of bulk electrical conductivity (σ_a) are used to determine the mass flux of solute past the ends of the TDR probes. In a simple approach, σ_a is related to the impedance load of the TDR probe (Nadler et al., 1991):

$$\sigma_a(t) = k\, Z^{-1}(t) \qquad [1]$$

where Z(t) is impedance load of the TDR probe at time t, and k is a calibration constant. Measurements of Z(t) obtained by TDR are a function of soil water content, θ, and electrical conductivity of the soil solution, σ_w. A linear relationship is generally observed between the resident solute concentrations, C (kg m^{-3}), and σ_a for constant water contents and for salinity levels ranging from 0 to $\approx$50dS m^{-1} (Ward et al., 1994). It is assumed that a vertically installed

TDR probe to depth L can measure the total amount of solute between x=0 (soil surface) and x=L at time t, regardless of the distribution of the solute along the probes (Kachanoski et al., 1992). After a solute pulse of tracer has been applied, the relative mass of applied tracer can be measured (Kachanoski et al, 1992) by

$$M_R(t) = \left[\frac{Z(t)^{-1} - Z(t_i)^{-1}}{Z(t_o)^{-1} - Z(t_i)^{-1}} \right] \qquad [2]$$

where $M_R(t)$ is relative specific mass of applied tracer at time t, Z(t) is impedance load of the TDR probe at time t, $Z(t_i)$ is impedance load before tracer application, and $Z(t_o)$ is impedance load after the specific mass of tracer application, but before any solute has moved past L. Detailed descriptions of Eq. [2] can be found in Kachanoski et al. (1992). This approach assumes that i) solute application must be completed before any of the applied solute passes the end of the probe rods, ii) the distribution of solute along the probe has no influence on Z^{-1} as long as all the applied solute is above the end of the TDR probe. Based on these assumptions and Eq. [2], the relative mass remaining within depth L at any time can be obtained. From the observed residual mass BTC using TDR, we can obtain a flux-averaged concentration BTC by taking the first derivative of $M_R(t)$ in Eq. [2] with respect to volume of outflow. Based on this TDR technique, one can easily determine solute transport properties with minimum disturbance of soil. The vertical probe approach by Kachanoski et al.(1992) is well suited to in situ measurements in heterogeneous systems and undisturbed soil cores because this method does not need a separate calibration experiment. In this study, we further tested whether the TDR method could be used to detect swine manure transport in soil.

Laboratory study

A soil column study was performed using manure as a tracer to test the applicability of TDR for manure transport measurements.

1. Soil column preparation and TDR setup

Undisturbed soil cores were collected from the Agronomy and Agricultural Engineering Research Center. The soil is classified as Nicollet silt loam (fine-loamy, mixed, superactive, mesic Aquic Hapludoll) in the Clarion-Nicollet-Webster soil association and has a weak fine subangular blocky structure. Nicollet soils were formed on uplands from glacial till and have a slope of 1 to 3%. Selected chemical and physical properties of the soil and experimental conditions of the soil cores are listed in Table 1. Everts and Kanwar (1990) and Jayachandran et al. (1994) reported preferential movement of both reactive and non-reactive solutes in this field. To obtain undisturbed soil cores from the field, 50-cm-wide and 40-cm-deep trenches were dug. For each soil core, a furnace pipe (so-called stove pipe, 12 cm diam. and 30 cm length), whose side was crimped and folded so that it could be opened from the side, was placed on the surface after removing vegetation. Soil around the pipe was gently shaved to form a pedestal approximately 12 cm in diameter. The pipe was then carefully pushed downward to encase the column and to avoid smearing. The process continued until 25-cm-long soil columns were obtained. The upper surface

of each soil column represented the actual field soil surface, with the exception that litter and loose soil had been carefully removed to provide a level surface.

In the laboratory, each furnace pipe was opened from the sides and removed from the undisturbed soil core. The soil cores were trimmed to the desired dimensions (10 cm diam. and 20 cm length). A polyvinyl chloride (PVC) plastic pipe (14 cm diam.) was put around each soil column so that the soil core was at the center of the PVC pipe. The space between the soil core and the PVC pipe was filled with molten paraffin wax to prevent solute flow along the wall. A wire screen was attached to the bottom of each column and a funnel was positioned beneath each column. A funnel was used to direct effluent to a fraction collector.

A 2.5-mm-diam. and 200-mm-long, two-wire type, baluned probe (Midwest Special Services, Inc., St. Paul, MN) was used for this study. A cable tester (model 1502B, Tektronix Corp., Redmond, OR) and TACQ program (Evett, 1998) were used to obtain Z and M_R as a function of time during miscible displacement experiments. The length of the coaxial cable was 150 cm and the experiment was conducted at a constant temperature of 25 ± 1 °C. In order to obtain Z, the simplified waveform analysis approach presented by Wraith et al. (1993) was used. The probe was installed vertically at the center of the soil column from soil surface to the bottom end of the soil column. Thus, we assumed that the TDR probe detected the total amount of tracer along the TDR probe regardless of the distribution of the tracer.

2. Miscible displacement experiments

Three undisturbed soil columns were used for the miscible displacement study. The soil columns were designated Column A, Column B, and Column C. Each soil column was mounted vertically and slowly saturated from the bottom with a background solution of 0.001 M $CaCl_2$. After saturation, TDR probes were vertically installed by carefully pushing them down through the soil surface. The bottom of each soil column was then opened for free drainage and steady flow with 1-cm surface head was established by applying about 10 pore volumes of 0.001 M $CaCl_2$ solution. Physical and chemical conditions of the soil columns are shown in Table 1. A steady-flow miscible displacement experiment was conducted to obtain a residual mass BTC using a pulse of manure application and TDR. Swine manure samples were obtained from the pits of 10,000-head hog confinement facility of Bisland Farm located in Madrid, Iowa about 40 km southwest of Ames. The samples were placed in a sealed plastic buckets to minimize excessive NH_3 volatilization and were subsequently stored at 5 °C. A 30 mL of swine manure was quickly applied at the top of each saturated soil column, and the effluent was collected at an interval of 0.05 pore volumes. Effluent breakthrough curves (BTC) were obtained based on electrical conductivity (EC) and concentrations of ammonium nitrogen (NH_4-N) and molybdenum reactive phosphorus (PO_4-P, MRP).

In order to calculate $M_R(t)$ in Eq. [2] from TDR measurements, the initial impedance load, $Z(t_i)$, of the soil solution was measured by TDR. The input impedance load, $Z(t_o)$, was measured right after the swine manure application but before any solute had moved out of the bottom of the soil columns. Each soil column was then leached with background solution (0.001 M of $CaCl_2$). Z(t) was measured at a time interval equivalent to 0.05 pore volume. $M_R(t)$ was obtained from

measured $Z(t_i)$, $Z(t_o)$, and $Z(t)$ values using Eq. [2]. Flux-averaged concentration BTC was then computed based on the $M_R(t)$. To obtain the flux-averaged concentration BTC, the first derivative, $M_R'(t)$, was computed. This derivative was then converted to mass(t) by multiplying by the mass applied. Finally, the concentration was computed by dividing the computed mass by leachate volume. Each 0.05 pore volume of outflow was also collected with a fraction collector from the bottom of the column and stored at 4 ˚C before analysis. The EC, NH_4-N, and MRP were determined using an EC meter and a Lachat Quickchem 8000 automated analyzer (Lachat Instruments division, Zellweger Analytics; Milwaukee, WI). The TDR-determined BTCs and the effluent-determined BTCs were compared with each other.

Lysimeter Study

Two field lysimeter experiments were conducted at the Agronomy and Agricultural Engineering Research Center of Iowa State University, about 11 km. west of Ames, Iowa. The soil at the site and in the lysimeters is Nicollet silt loam. The lysimeters are non-weighing types with a width of 0.97 m, length of 2.28 m and a depth of 1.35 m and has a built-in vertical water withdrawal tube connected to a 0.1 m-diameter perforated drainage pipe laid horizontally at the bottom of the lysimeter. The experimental set-up consists of a 3785-liter water tank with built-in flow regulator as water source for ponding the lysimeter and an impeller pump for collecting effluent samples from the drain at the lysimeter bottom. Sixteen (16) TDR probes ranging in length from 15 cm to 60 cm were installed vertically in the lysimeter in two rows and are spaced about 0.25 m apart on the average. All probes were made of stainless steel and connected with a coaxial cable. The 15-cm probes are two-rod probes built with a balun while the 60 cm probes are three-rod probes without a balun. The 30-cm probes were either two-rod or three-rod probes. The probes were connected to a multiplexer and a cable tester. A total of 16 TDR probes were used in each experiment. The most essential details of the lysimeter experiments are shown on Table 2.

The experiments were performed under saturated flow conditions in early fall of 1999. The lysimeter was initially saturated from the bottom using 0.001 M $CaCl_2$ background solution in order to satisfy the requirements for linearity between the soil bulk electrical conductivity and soil-water electrical conductivity. Prior to the actual experiments, the lysimeters were tested for leakage occurrences to ensure a more accurate effluent sampling. The tests were made under dynamic conditions simulating the actual conduct of the swine manure transport experiments. Results indicated leakage rates averaging less than 5 % of the total inflow. Swine manure was applied uniformly over the surface of the lysimeter at a rate approximately equal to actual farm application rates of about 7500 L/ha using sprinkler cans to screen the large solid contents of the slurry and prevent excessive surface clogging during application. The surface was ponded at a constant head of about 6.5 cm. After the manure has infiltrated, effluent samples with a volume of about 150 mL were collected every 34 L, representing about 1/40 of the pore volume of the lysimeter. The experiments were performed until about 2 to 3 pore volumes were collected. The samples were brought to the laboratory for EC analysis. The EC of the applied swine manure averaged 11.8 and 15.35 mmhos/cm while the background electrical conductivity values prior to the swine manure application were 0.83 and 0.37 mmhos/cm for the first and second experiments, respectively. The average flow rates were 0.09 and 0.05 L/s for the first and second experiments respectively. Sampling intervals for effluent collection were the same for both experiments at 1/40

pore volumes.

Effluent samples were analyzed for electrical conductivity and relative residual mass breakthrough curves (BTCs) were generated. On the other hand, the waveform data obtained from TDR measurements were converted to impedance load using the simplified waveform analysis by Wraith et al (1993) and were consequently transformed into relative residual mass using the method developed by Kachanoski et al (1992). The relative mass breakthrough curves obtained from both direct effluent and TDR measurements were then compared to evaluate the feasibility of the TDR method for predicting swine manure transport.

Results and Discussion

Laboratory Study

Figure 1 shows effluent BTCs of EC obtained from Column A along with calculated BTCs obtained from TDR. In general, the BTCs for all soil columns showed very early arrival and tailing which is representative of preferential flow or physical nonequilibrium processes. The TDR-calculated BTCs were similar to the measured effluent BTCs. The results were similar for Column B and Column C. Similar findings were reported by Lee et al. (in press).

Figure 2 shows effluent BTCs of NH_4-N and MRP from the miscible displacement experiments. the BTCs of NH_4-N and MRP also showed preferential flow with an early breakthrough and tailing. Mass recovery of NH_4-N and MRP calculated based on the effluent BTCs ranged from 2.1 to 5.8 % and from 3.3 to 6.0 %, respectively. The results imply that most of the NH_4-N and MRP was sorbed to soil, and only a small portion of the compounds were passed through the soil column.

Main compounds of the swine manure used in this study were chloride, nitrogen, and phosphorus, and chloride was the main compound that dominated EC of the liquid swine manure. Because the TDR-determined BTCs were based on the bulk EC of the soil, the TDR-determined BTCs were several magnitude higher than the measured BTCs of NH_4-N and MRP, while the TDR-determined BTCs were similar to the measured EC BTCs. However, the time of the peak for the both TDR-determined BTCs and measured NH_4-N and MRP BTCs was almost identical, implying that the TDR-determined BTCs can detect the most vulnerable time for the N and P leaching. For example, peak of the NH_4-N and MRP BTCs for Column A were 0.22 and 0.24 pore volumes, respectively, and peak of the TDR-determined BTCs was at 0.22. Although TDR could not generate the same scale of measured BTCs for N and P, TDR showed a feasibility to predict the peak of the BTCs so that one can use TDR as a tool to make first approximation of leaching of N and P in soil, especially when preferential flow exists.

Lysimeter Study

The first field experiment was performed using an alternating current (AC) electrical power source to power the laptop computer hooked up to the TDR cable tester and multiplexer. The

latter components were powered by a direct current (DC) 12-volt car battery. Although the expected waveform showed up in the monitor of the cable tester during the instrumental set up and actual TDR measurements, the calculated values of impedance load showed some degree of distortions when plotted against time or pore volume. A sample of these results is shown on Figure 3. This finding was hypothesized to be caused by electromagnetic interference upon using an AC power source to power any of the components of the TDR data collection system. This hypothesis was tested and confirmed in a second experiment when a gasoline fueled generator of alternating current was used for the laptop computer and a car battery for the cable tester and multiplexer. Better TDR results were obtained with the change in power supply in terms of noise elimination in the calculated values of impedance load. A sample result is shown in Figure 4 for probe 12, the same probe depicted in Figure 3. This probe also yielded the best TDR data. These findings are significant and useful for prospective TDR users performing field experiments in areas where possible electromagnetic wave interference exists. Although the TDR data with some degree of noise could still be rendered useful as long as some trend was evident by employing some smoothing techniques such as non-linear regression as was done in this study, using DC power supply would eliminate this additional filtering process.

The impedance load values obtained from the experiments were calculated using the simplified waveform analysis proposed by Wraith et al. (1993) on the basis of the voltage readings obtained using the TACQ program. For both experiments, a total 10 TDR probes yielded fairly acceptable TDR data based on impedance load trends and these were chosen for the subsequent analysis. The poor performance of the remaining probes may be attributed to electrical interference in the field and poor contact of the probes with soil.

The data normalization method in Eq. [2] was used to transform the impedance load values into relative residual mass values as a function of time (or pore volume). Results generally yielded the expected declining trend with time. These results were further discussed and depicted in the latter section on comparison between TDR and direct effluent measurements.

A sample plot of the EC against pore volume is shown in Figure 5. Noticeable in Fig. 5 is the early breakthrough of swine manure at the bottom of the lysimeter with the peak EC occurring as quickly as 0.12 pore volume. In the other experiment, the peak EC occurred at about 0.25 pore volume. This early breakthrough may be attributed to preferential flow in some parts of the lysimeter. During the preparation stage of the experiments, cracking of the soil in the lysimeter was observed as a result of wetting and drying due to intermittent rainfall occurrences. Hence, preferential flow was likely to have occurred during the actual experiments.

Plots of the relative residual mass obtained from TDR and direct effluent measurements are shown in Figures 6 and 7. The relative mass breakthrough curves based on the TDR results from the first experiment for the selected probes are nearly identical due to the smoothing effect applied to the TDR data, as previously discussed. Nevertheless, it is important to note that the TDR results yielded lower relative mass at increasing pore volumes beyond one pore volume compared to direct effluent measurements. This is valid since the length of the TDR probes is shorter than the total depth of the lysimeter. Hence, while swine manure has leached past the probe length, thereby making the relative mass approach zero, there are still some residual swine manure contained in

the lower portion of the lysimeter below the probes making the residual mass from direct effluent measurements relatively greater than that from TDR data.

The same trends were demonstrated in the second lysimeter experiment as shown in Figure 7. However, without the need for smoothing the TDR data, the generated relative mass BTCs in this experiment appeared to be more representative of the EC changes that took place within the vicinity of the probes. Of the 30-cm probes used, probe number 12 provided the best quality data in terms of impedance load. Hence this probe is the most appropriate to use for comparative purposes. As shown in Figure 7, the relative mass from the probe 12 (L= 30 cm) declined faster than the 60-cm probe. This is again valid as it obviously takes a longer time for swine manure to move past the 60-cm long probe than its shorter counterpart. Hence, while swine manure had gone past the 30-cm probe, its presence was still detected by the 60-cm probe making the residual mass of the latter greater than in the former at increasing pore volumes or times. Similar to the first experiments, TDR data from all probes generated earlier decline in the relative residual mass than from effluent data. This is again due to the aforementioned difference between the probe length and the lysimeter depth. Despite some imperfections, the results of this study demonstrated the potential in using TDR for swine manure transport monitoring.

Overall, the effluent data showed an early breakthrough of swine manure in terms of EC, with the effluent EC peaking from 0.12 and 0.25 pore volumes. The resulting breakthrough curves generally followed the typical behavior of breakthrough curves although a double hump was exhibited in the second lysimeter experiments on soils with cracks. These findings further demonstrate the major role contributed by preferential flow due to soil cracks in the leaching of swine manure in soils. For the TDR results, a total of 10 probes yielded relatively high quality data yielding the expected impedance load behavior against time or pore volume. The various lengths of probes, however, generated TDR data that yielded realistic relative residual mass breakthrough curves that agreed fairly with those obtained from direct effluent measurements. The TDR data resulted to an earlier decline in the relative residual mass with increasing time or pore volume compared to that from effluent data. This is valid since the length of the probes used is shorter than the lysimeter depth. The TDR technique showed some potential in replicating the relative residual mass breakthrough curve of swine manure.

Conclusions

Time domain reflectometry technique was tested on swine manure transport measurements using undisturbed soil cores in laboratory and lysimeters in field. For both laboratory and lysimeter studies, preferential flow was evident in the experiments with the occurrence of early breakthrough and tailing of swine manure. Despite the occurrence of preferential flow, the TDR data obtained from 15 to 60 cm probes still yielded realistic relative residual mass breakthrough curves. TDR-determined breakthrough curves (BTCs) generally yielded similar trends as the BTCs obtained from direct measurements of electrical conductivity of effluent samples, and the time of peak for the TDR-determined BTCs and the NH_4-N and PO_4-P BTCs was very similar. The result showed a potential for using TDR for monitoring swine manure transport for groundwater quality studies. Overall, this study has initiated an important step in exploring the applicability of TDR technique in groundwater quality monitoring as a result of swine manure field application. Results of this study may serve as a framework for further field studies using

TDR.

Basic Information

Title:	Microcystin-LR: a potential contaminant of concern for Iowa surface waters
Project Number:	B-05
Start Date:	3/1/2000
End Date:	2/28/2002
Research Category:	Not Applicable
Focus Category:	Toxic Substances, Surface Water, Nutrients
Descriptors:	microcystin, cyanobacteria, water quality, lakes
Lead Institute:	Iowa State Water Resources Research Institute
Principal Investigators:	Maureen E. Clayton

Publication

1. Schultz, Alissa C., Leah C. Osterhaus, Edward J. Brown and Maureen E. Clayton. March 2001. Microcystin-LR: A Potential Contaminant of Concern for Surface Water Quality in Iowa. A poster presentation at the Agriculture and the Environment: State and Federal Water Initiatives workshop, Ames, IA.
2. Schultz, Alissa C., Leah C. Osterhaus, Edward J. Brown and Maureen E. Clayton. April 2001. Microcystin-LR: A Potential Contaminant of Concern for Surface Water Quality in Iowa. A poster presentation at the UNI Sigma Xi Student Research Conference, Cedar Falls, IA.

Introduction

Surface water quality is currently one of the most important environmental issues facing the state of Iowa because the ecological, recreational and aesthetic values of these water bodies are threatened by non point source (NPS) pollution. The traditional threat to lake water quality from NPS contaminants is eutrophication resulting from nutrient loading. Preliminary evidence from a study of two Iowa lakes by a multidisciplinary team of researchers at the University of Northern Iowa, however, indicates that algal species composition may also be altered by nutrient loading. The dominance of cyanobacteria in eutrophic lakes suggests that water quality and human and wildlife health may be endangered by exposure to toxin producing strains of cyanobacteria.

Summer blooms of cyanobacterial populations are common in eutrophic lakes and ponds. These blooms represent very high concentrations of cyanobacteria in the water column, and may result in a discoloration of the water and in the formation of what is colloquially known as "pond scum". Blooms are initiated and exacerbated by factors including excessive nitrogen (N) and phosphorus (P) loading, surface water temperatures $> 20\ ^{o}C$, stratification of the water column, long water residence time, organic matter enrichment, low total and dissolved N:P ratios, and high irradiance and long daylength. These conditions are common in Iowa lakes and ponds, especially those which are impacted by nutrient loading from agricultural runoff.

High cyanobacterial concentrations may reduce recreational use of surface waters because of the aesthetic impact of the discolored water. In addition, some species of cyanobacteria produce biotoxins that can result in severe health impacts and death in humans and wildlife. Microcystin-LR is the most toxic of the cyanobacterial biotoxins; it is known to be a potent inhibitor of protein phosphatases 1 and 2A (Toivola et al 1994, Runnegar et al 1995, Sahin et al 1995, Craig et al 1996), as well as a tumor promotor (Lam et al 1995). Neurotoxic illness and liver failure have been observed in exposed humans (Jochimsen et al 1998, Pouria et al 1998). Microcystin-LR may also be transferred through the food chain (Kotak et al 1996, Prepas et al 1997) and can result in sublethal effects, including ionic imbalance, decreased grazing, and reduced growth, in fish and other aquatic organisms (Beveridge et al 1993, Keshavanath et al 1994, Bury et al 1995).

Recent research on microcystin-LR has primarily focused on the following areas: (1) laboratory experiments to elucidate the mechanism of action (e.g. Toivola et al 1994, Lam et al 1995, Runnegar et al 1995, Sahin et al 1995, Craig et al 1996), (2) laboratory studies to examine the effects of nutrients on toxin production (e.g. Parker et al 1997, Rapala et al 1997), (3) improved analytical methods for toxin detection (Lambert et al 1994, Lin and Chu 1994, Liu et al 1996, Ward et al 1997), and (4) mechanisms of toxin degradation (Tsuji et al 1994, Bourne et al 1996). This research suggests that cyanobacterial toxins may be environmentally relevant contaminants if toxin-producing strains are abundant, or if the strains are exceptionally toxic.

Species that are known to produce microcystin-LR (*Microcystis* sp. and *Anabaena* sp.) have been observed as dominant members of the phytoplankton assemblage in two

Iowa lakes, Silver Lake and Casey Lake (Osterhaus 1999). Unfortunately, however, toxic and non-toxic strains are difficult or impossible to distinguish morphologically (Boney 1975). A direct competitive ELISA using antibodies against microcystin-LR (Lin and Chu 1994, Liu et al 1996) is now available to quantitatively determine the microcystin concentration in surface waters. We used this ELISA to determine the degree of the potential threat posed by microcystin-LR to the health of the humans and wildlife (as well as the ecosystem) that utilize two Iowa lakes. The primary objective of the study was to determine the potential threat from cyanobacterial toxins by determining the toxin content in surface waters and correlating these concentrations to cyanobacterial abundance and species composition, and therefore indicating whether or not microcystin-LR should be considered as a contaminant of concern in surface waters. Nutrient concentrations were also determined in the lakes because the nutrients N and P may stimulate cyanobacterial growth, while increased P is correlated with increased microcystin concentration within the cell (Rapala et al 1997); both pathways (increased cyanobacteria populations and increased toxin content per cell) will result in increased toxicity within the water column. The results of this research will provide information to assist resource managers in determining the extent of the problem and in suggesting the need for novel remediation strategies for hypereutrophic Iowa lakes.

Materials and Methods

Two lakes in northeastern Iowa were chosen for this study. Silver Lake, located in the town of Delhi (Delaware County – 42°25'N, 91°19'W), is heavily impacted by land use practices within the watershed, which are primarily agricultural (81% cropland and small hog farms); a small residential area and school ball fields also border the lake. Silver Lake does not currently support its designated use as a recreational water body; winter fish kills are common, stocked fish do not thrive, and cyanobacterial blooms discolor the water. The Iowa Department of Natural Resources has installed an aerator as a remediation effort, but this attempt has been unsuccessful to date. On the other hand, Casey Lake, located in Hickory Hills Park (Tama County – 42°16'N, 92°19'W), is located in a watershed that is primarily parkland (58%), although there is agricultural activity in the form of cropland (31%) within the watershed. The entire shoreline is publicly owned. The lake supports a thriving recreational fishery, including ice fishing tournaments. Fishing, swimming, picnicking, and camping are common recreational activities around the lake.

Both lakes are relatively small and shallow and originated as impoundments. Casey Lake is the larger of the two, with an area of 54 acres and a mean depth of 3.1 m (maximum depth 7.6 m). Silver Lake is approximately 34 acres in area, with a mean and maximum depth of 1.9 and 4.6 m, respectively. The watershed of Silver Lake is smaller, at approximately 5.4 times the area of the lake, while Casey Lake has a watershed area that is 13.6 times the area of the lake (Bachman et al 1994). Casey Lake has three permanent inflows, while Silver Lake is fed entirely by precipitation and runoff. The volume of both lakes is controlled by gated outflows.

Water samples were collected weekly from June 20th to August 10th at stations located along a series of transects within the body of Silver Lake and Casey Lake in conjunction

with the UNI Lake Water Quality Study. During sample collections, *in situ* measurements of dissolved oxygen, temperature, turbidity and secchi disk depth were conducted. Samples for microcystin analyses were collected weekly from the surface in acid rinsed sterile bottles from 14 stations in Casey Lake and 10 sites in Silver Lake. The samples were transported to the laboratory on ice, where they were stored at 4 ^{o}C and processed as soon as possible. In the lab, phytoplankton cells were separated from lake water by centrifugation (Silver Lake) or gravity filtration (Casey Lake). Cell lysate was obtained by centrifugation after sonication in phosphate buffered saline, pH 7.2 (McDermott et al 1995). The lake water (cell free) and cell lysate samples were stored at -20ºC.

Lake water samples were also collected for the analysis of chlorophyll *a* concentrations and determinations of phytoplankton species diversity. Water samples for chlorophyll *a* analyses were collected from the surface at the same stations as for microcystin analysis and transported to the laboratory on ice, where they were stored at 4^{o}C prior to analysis. Chlorophyll *a* was extracted in 90% acetone from water samples filtered through glass fiber filters, and then measured spectrophotometrically by a method that corrects for the presence of phaeophytin, a chlorophyll *a* degradation product (Clesceri et al 1998). Phytoplankton samples were collected from two sites within the body of each lake with an 80 μm mesh plankton net. After being transported to the laboratory on ice, the samples were preserved in Lugol's solution for later analysis (Clesceri et al 1998). The phytoplankton were identified to the lowest possible taxonomic unit and were counted using a hemocytometer. Relative abundances of cyanobacteria and green algae were computed from the count data.

Microcystin-LR concentrations were determined in lake water and cell lysate samples by direct competitive enzyme linked immunosorbent assay (ELISA) (Lin and Chu 1994, Liu et al 1996), using kits purchased from EnviroLogix (Portland, ME). The kit is based on a monoclonal antibody developed against microcystin-LR. Other microcystins may cross react with the antibody to a lesser degree. Therefore, HPLC studies (McDermott et al 1995) are in progress to verify that the ELISA assay results are due to the presence of microcystin-LR in the samples. Until these analyses are completed, the data will be reported as concentration of microcystin.

The results of the chlorophyll *a* analyses were used to select samples for toxin analysis. For each sampling date, three samples were selected from each lake; these samples corresponded to a station at or near the mean chlorophyll *a* concentration in the lake on that date, as well as the stations with the highest and lowest chlorophyll values. This approach was selected in order to adequately characterize the spatial and temporal variation in the lakes without the prohibitive expense of analyzing each sample. Purified microcystin-LR standards were run on each plate along with the lake samples. Each sample (standards, lake water and cell lysate) was analyzed in triplicate; mean microcystin concentrations and standard deviations are reported. Lake water samples are reported as μg microcystin/L, and cell lysate toxin concentrations are reported as μg microcystion/mg cells (wet weight).

Lake water samples were also collected at each station and transported to the laboratory in acid rinsed bottles on ice for nitrate and phosphate analysis. Nitrate concentrations were measured with an ion selective electrode (Vernier, Beaverton, OR). Unfortunately, this method proved to be unreliable, occasionally producing erroneously high nitrate values; this data will, therefore, not be presented. Total phophorus was measured by the ascorbic acid colorimetric method after persulfate digestion (Clesceri et al 1998). Soluble reactive phosphorus was also determined after filtration of Silver Lake samples through 0.45 μm membrane filters.

Toxin concentrations in both cell free lake water and cell lysate samples were evaluated in relation to the other water quality parameters. Linear regressions were used to determine the statistical significance of the observed relationships.

Results and Discussion

Concentrations of microcystin in two Iowa lakes ranged from non-detectable levels (<0.16 μg/L) to more than 1.6 μg/L. Microcystin concentrations in Silver Lake were consistent during the sampling period (0.9 μg/L), and were always higher than concentrations at Casey Lake, where microcystin peaked from 7/20 to 8/2 (0.8 μg/L) before returning to background levels (0.2 μg/L) (Figure 1). These values are consistent with results from previous studies of lakes in Wisconsin (McDermott et al, 1995) and Alberta, Canada (Kotak et al, 1996). The observed concentrations are lower than those found to result in reduced growth of brown trout (41-68 μg/L – Bury et al, 1995). Even though these values would not appear to result in direct effects on fish populations, they are near the 48h LC_{50} for *Daphnia pulex* (1 μg/L – Reinikainen et al, 1994), suggesting that fish and other aquatic organisms could be impacted by effects at lower levels of the lake food web.

Microcystin concentrations in cell lysates ranged from 0.1 to 320 μg/g, and were always higher in Casey Lake (155 μg/g) than in Silver Lake (2 μg/g) (Figures 2 and 3). These values are consistent with the results of studies of cyanobacterial blooms (Jungmann and Benndorf, 1994 ; McDermott et al, 1995) and laboratory strains of *Microcystis* (Jungmann and Benndorf, 1994). The results suggest that a higher percentage of the phytoplankton in Casey Lake produce toxin, or that each toxin producing cell in this system makes more microcystin.

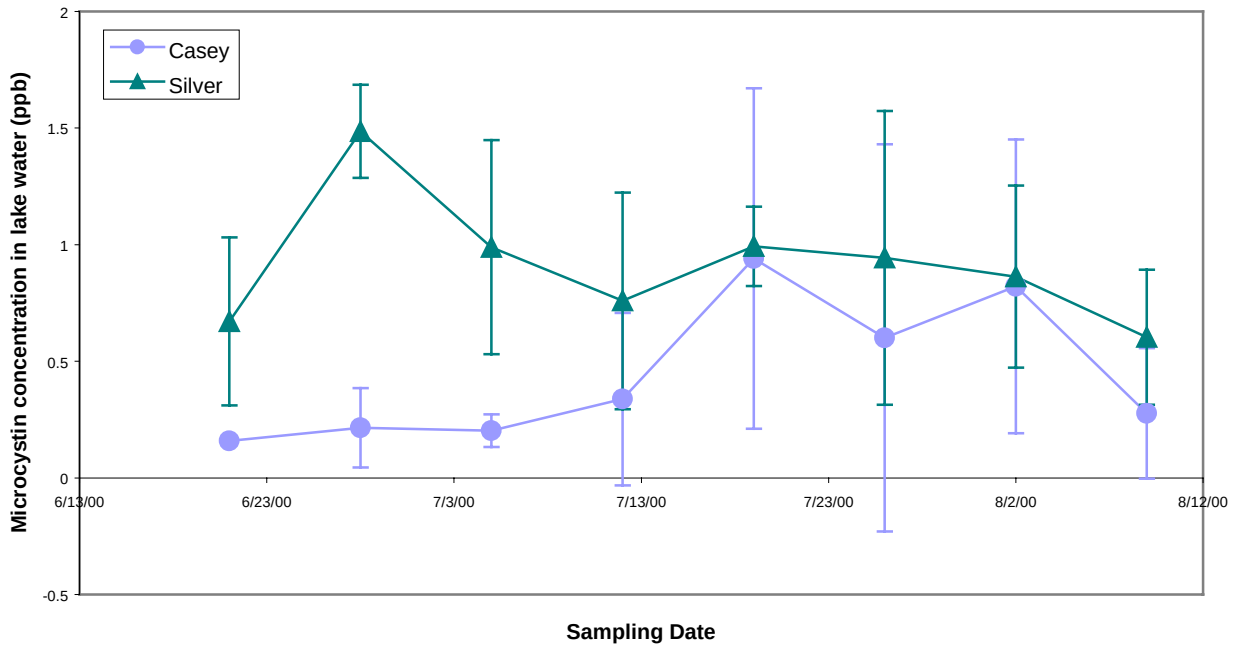

Figure 1. Temporal trends in microcystin concentrations in cell-free lake water samples. Means ± standard deviations are shown for Casey Lake in the circles and for Silver Lake in the triangles.

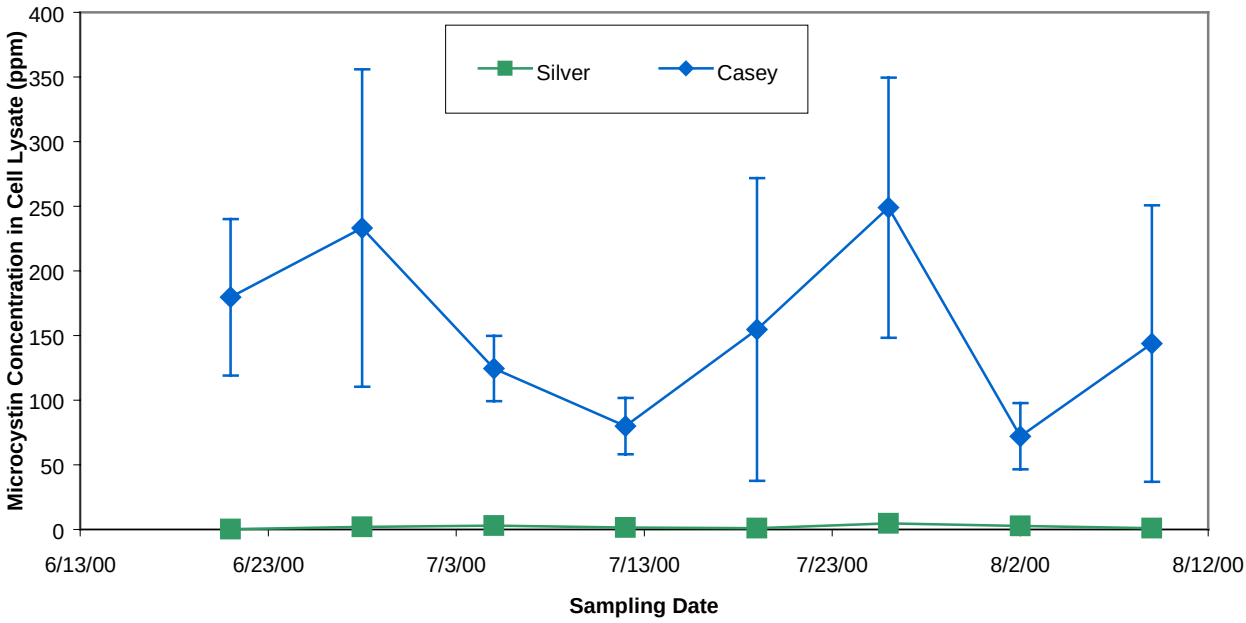

Figure 2. Temporal trends in microcystin concentrations in cell lysate samples, given as µg microcystin per mg cells (wet weight). Concentrations in cells (mean ± standard deviation) from Casey Lake are shown as diamonds; Silver Lake samples are shown as squares.

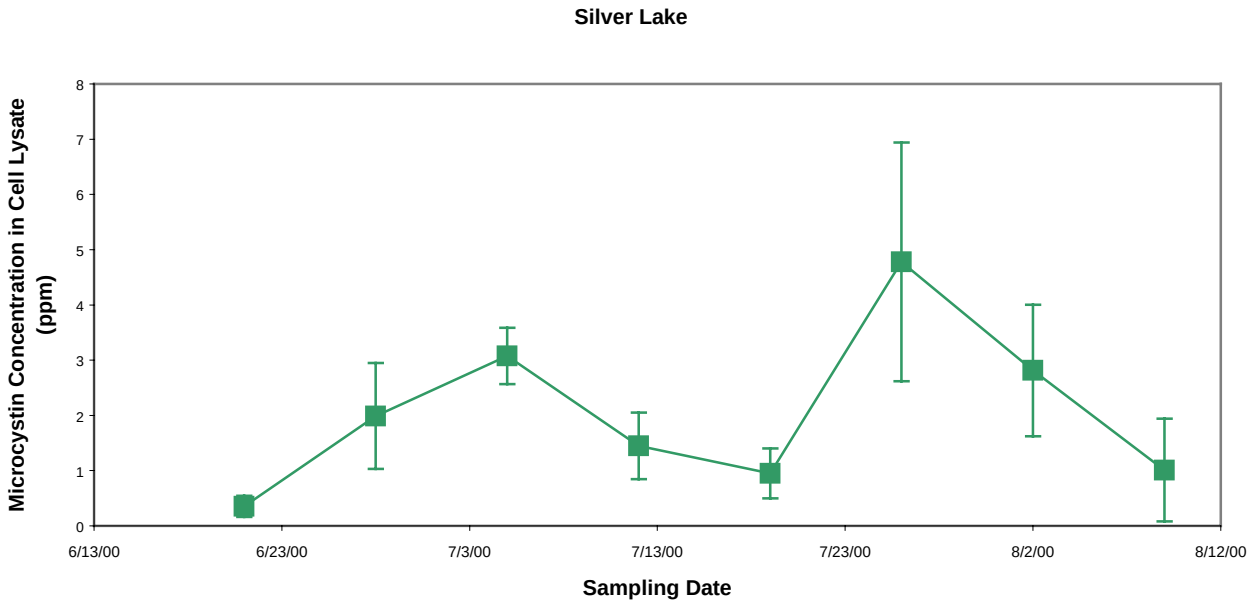

Figure 3. Temporal trends in microcystin concentrations (µg/mg wet weight) in cell lysate samples from Silver Lake phytoplankton. Note the difference in the scale of the y-axis from Figure 2.

There were no significant relationships between microcystin concentrations in lake water or cell lysate and chlorophyll *a* (Figures 4-7), relative cyanobacterial abundance (Figures 8-9), total phosphorus (Figures 10-13), dissolved oxygen (data not shown), turbidity (data not shown), secchi disk depth (data not shown), or water temperature (data not shown). In contrast, cyanobacterial toxin concentrations would be expected to correlate with cyanobacterial concentrations or other similar measures, and with nutrient concentrations in the water column. In fact, Rapala et al (1997) found increased concentrations of microcystin in *Anabaena* cells in culture with increasing phosphorus concentrations, but the examined concentrations (0.5-5 mg PO_4-P/L) were much lower than the values observed in Silver and Casey Lakes. Perhaps the cyanobacteria in these two lakes have sufficient nutrients and therefore these measures are no longer correlated with toxin production.

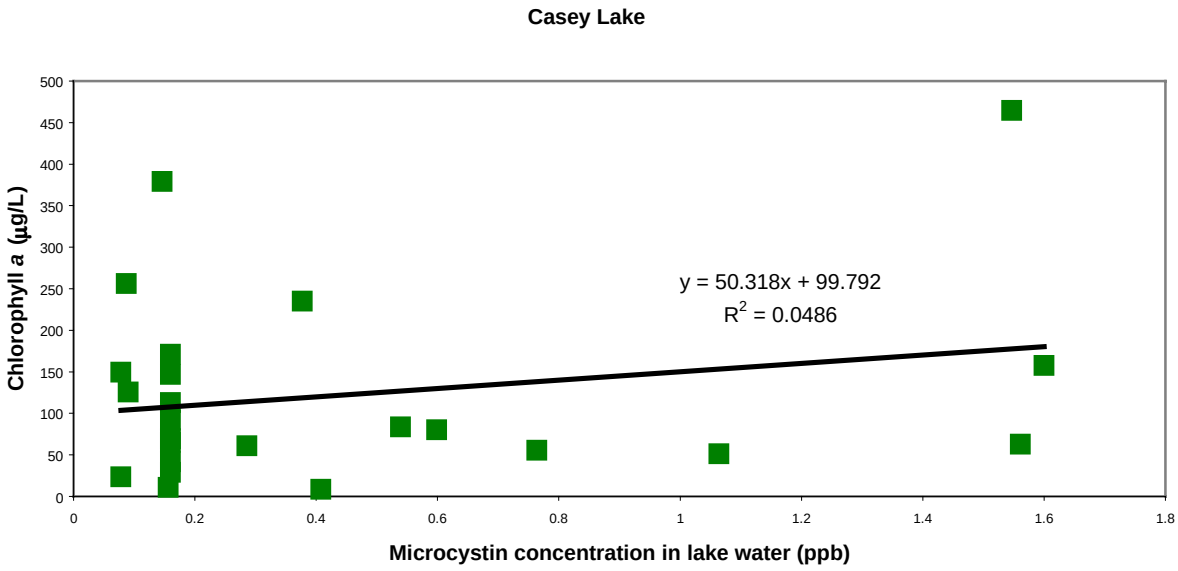

Figure 4. Microcystin concentrations (µg/L) in Casey Lake are not correlated (R^2=0.05) with lake phytoplankton populations measured by chlorophyll *a* concentrations (µg/L) in samples collected at the same time and station.

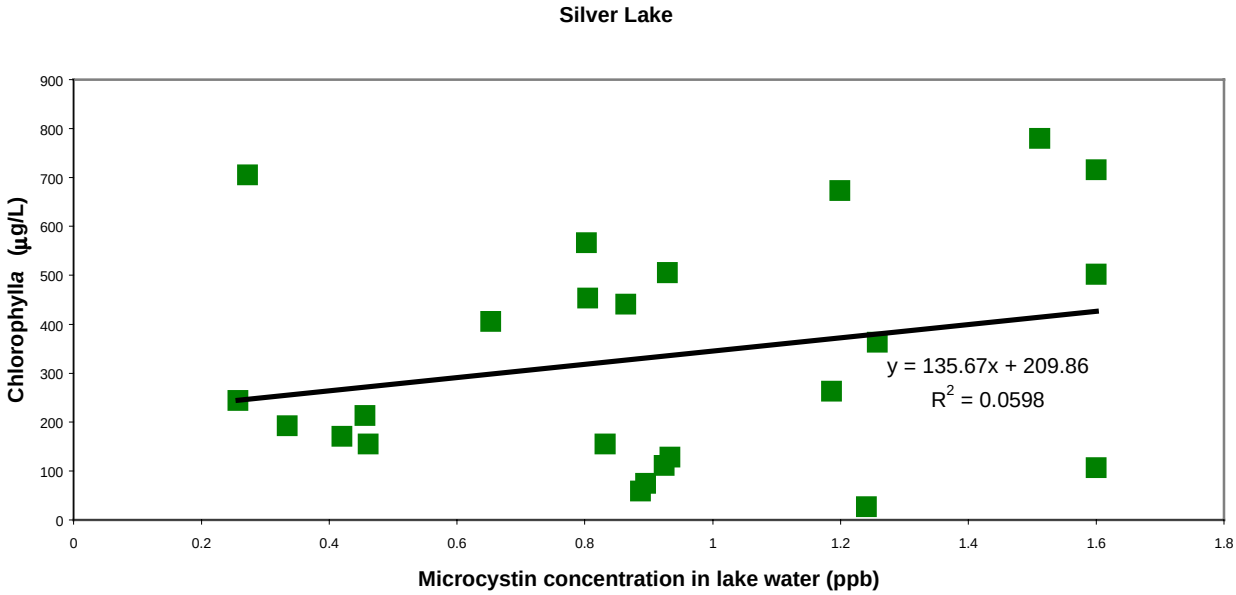

Figure 5. Microcystin concentrations (µg/L) in Silver Lake are not correlated (R^2=0.06) with lake phytoplankton populations measured by chlorophyll *a* concentrations (µg/L) in samples collected at the same time and station.

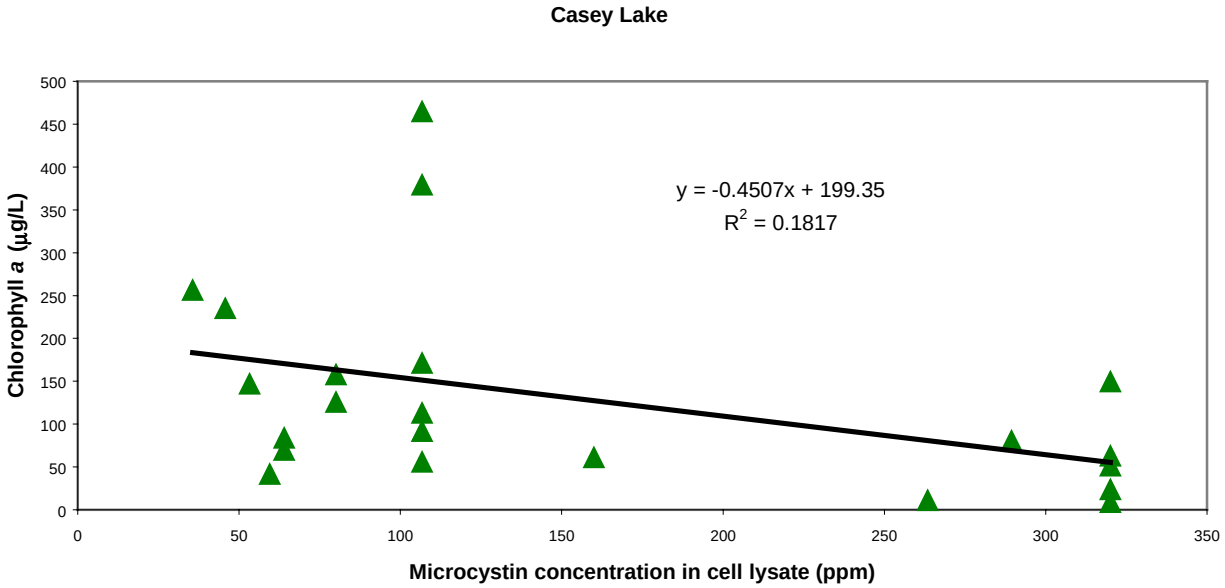

Figure 6. Microcystin concentrations (µg/mg) in cell lysate samples of Casey Lake phytoplankton are not correlated (R^2=0.2) with lake phytoplankton populations measured by chlorophyll *a* concentrations (µg/L) in samples collected at the same time and station.

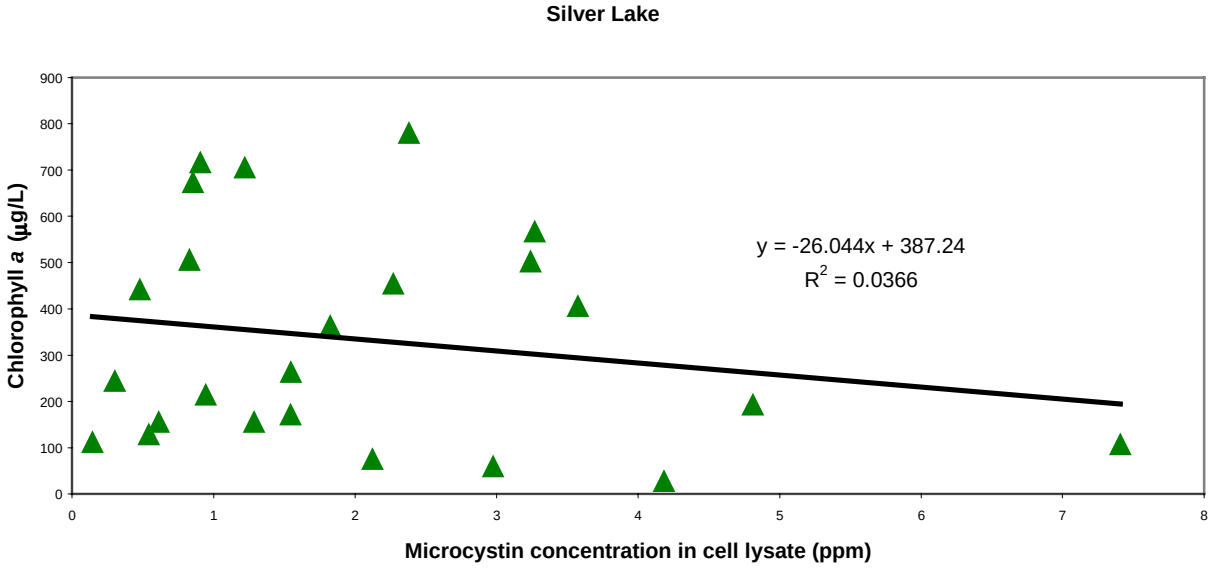

Figure 7. Microcystin concentrations (µg/mg) in cell lysate samples of Silver Lake phytoplankton are not correlated (R^2=0.04) with lake phytoplankton populations measured by chlorophyll *a* concentrations (µg/L) in samples collected at the same time and station.

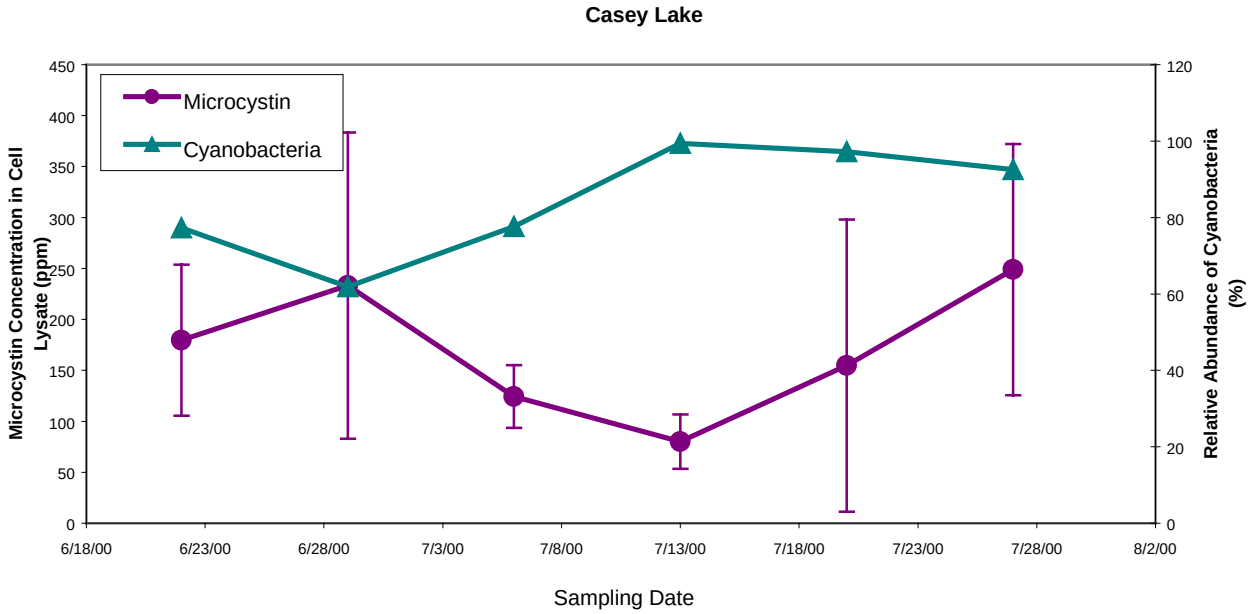

Figure 8. Temporal trends in microcystin concentrations (µg/mg wet weight) in cell lysate (circles; mean ± standard deviation) and relative abundance of cyanobacteria (triangles) in Casey Lake. Based on linear regression analysis (not shown), the relationship between the two parameters is not significant (R^2=0.2).

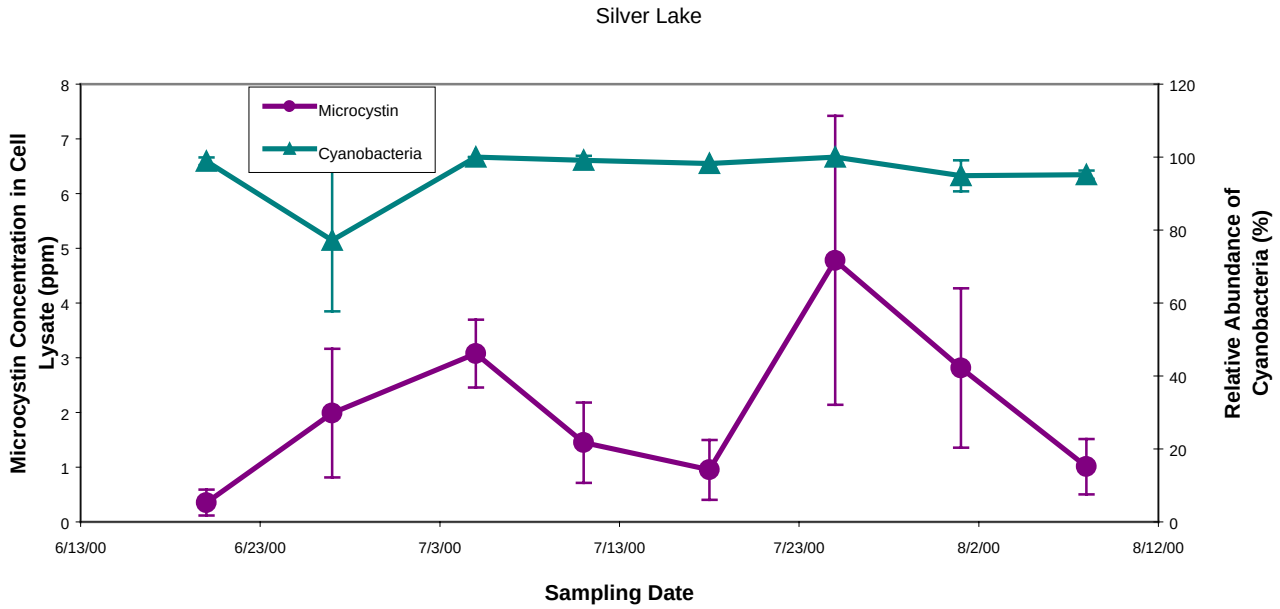

Figure 9. Temporal trends in microcystin concentrations (µg/mg wet weight) in cell lysate (circles; mean ± standard deviation) and relative abundance of cyanobacteria (triangles) in Silver Lake. Based on linear regression analysis (not shown), the relationship between the two parameters is not significant (R^2=0.01).

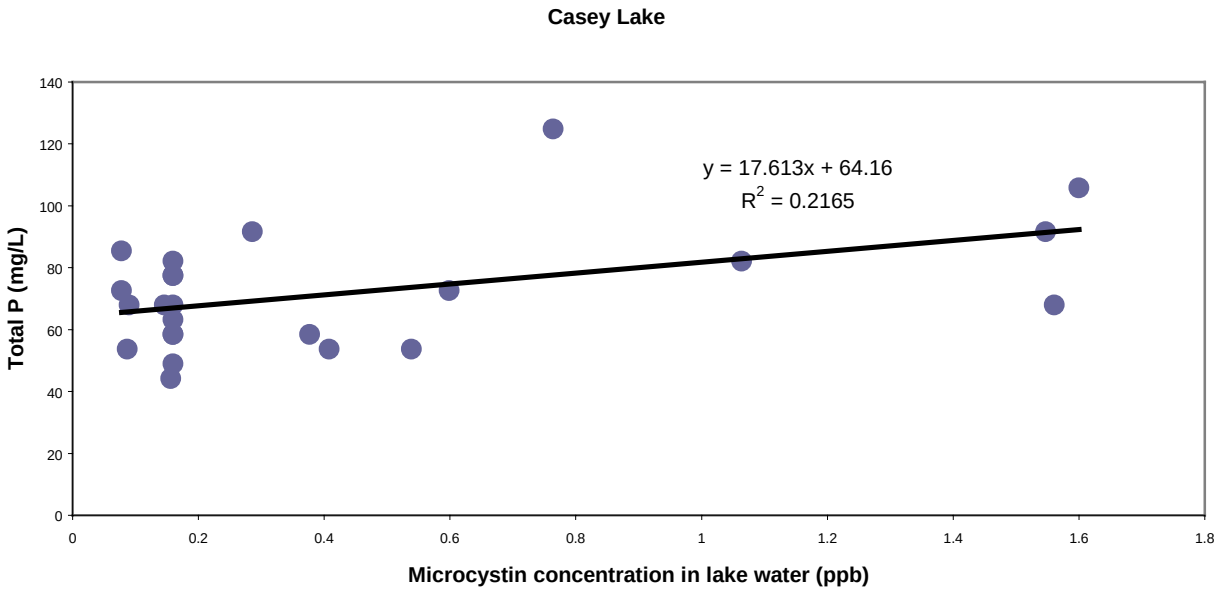

Figure 10. Microcystin concentrations (µg/L) in Casey Lake are not correlated (R^2=0.2) with lake phosphate concentrations measured as total phosphorus (mg/L) in samples collected at the same time and station.

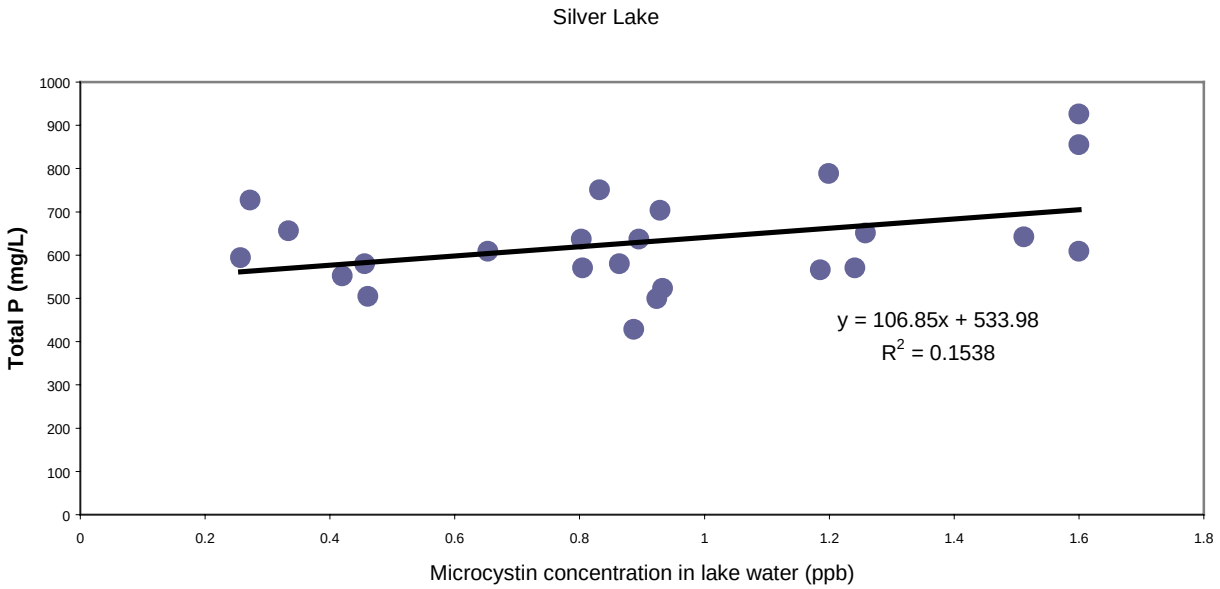

Figure 11. Microcystin concentrations (µg/L) in Silver Lake are not correlated (R^2=0.2) with lake phosphate concentrations measured as total phosphorus (mg/L) in samples collected at the same time and station.

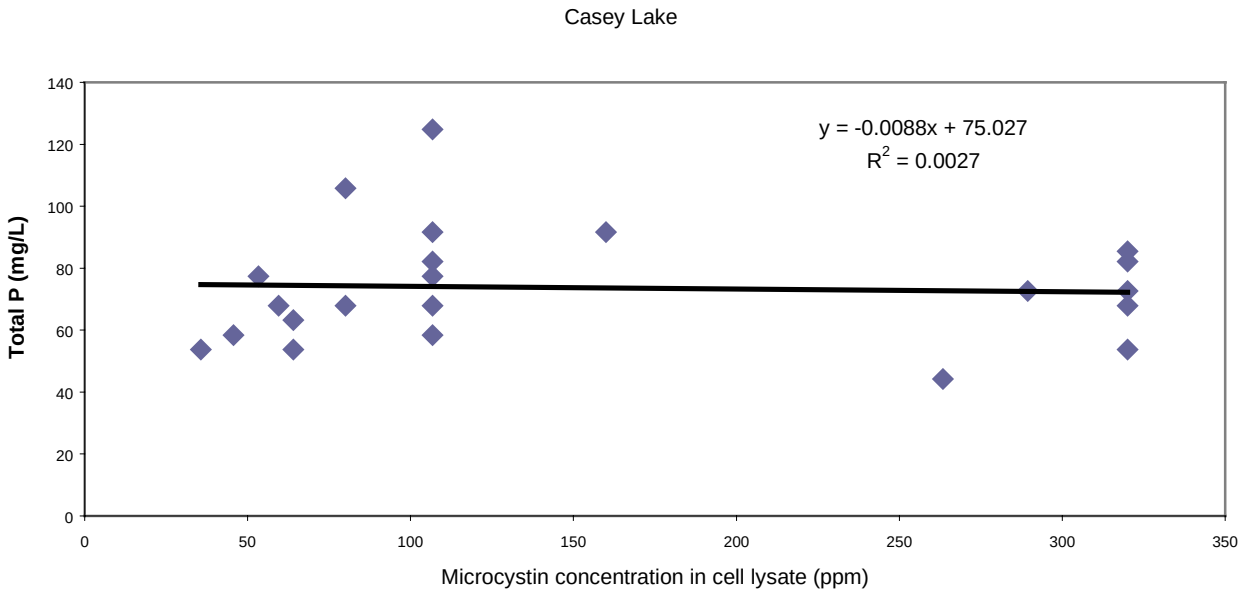

Figure 12. Microcystin concentrations (µg/mg) in cell lysate samples from Casey Lake are not correlated (R^2=0.003) with lake phosphate concentrations measured as total phosphorus (mg/L) in samples collected at the same time and station.

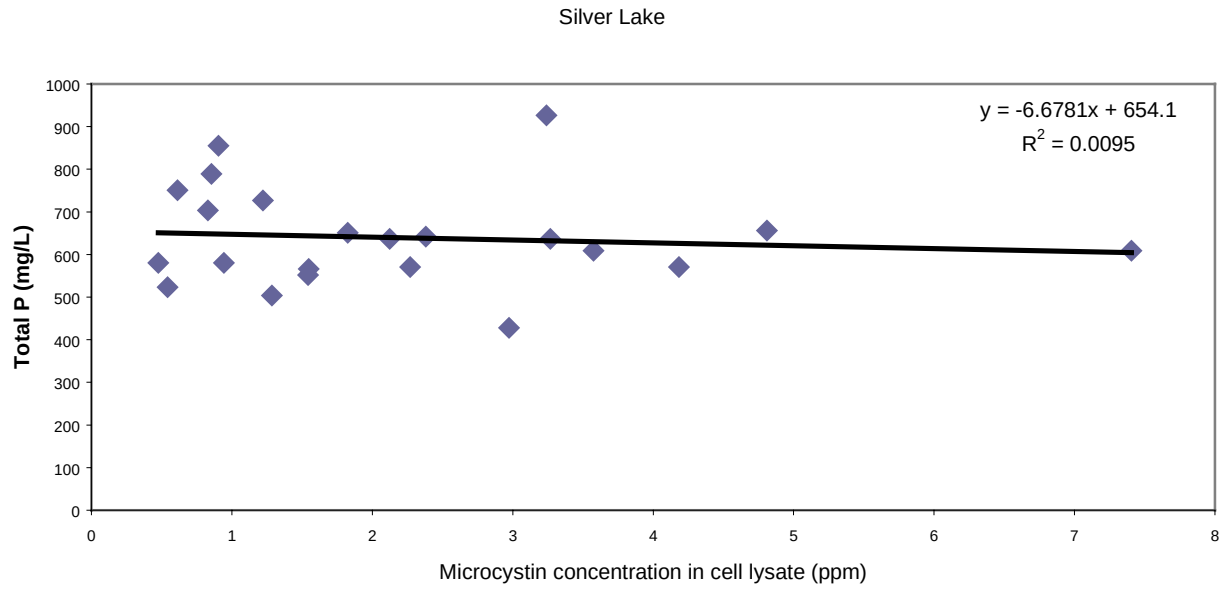

Figure 13. Microcystin concentrations (µg/mg) in cell lysate samples from Silver Lake are not correlated (R^2=0.01) with lake phosphate concentrations measured as total phosphorus (mg/L) in samples collected at the same time and station.

Conclusions

Concentrations of microcystin in Silver and Casey Lakes in the summer of 2000 ranged from non-detectable levels (<0.16 μg/L) to more than 1.6 μg/L, which is consistent with studies of lakes in Wisconsin and Alberta, Canada. Microcystin concentrations in Silver Lake were consistent during the sampling period (0.9 μg/L), and were always higher than concentrations at Casey Lake, where microcystin peaked from 7/20 to 8/2 (0.8 μg/L) before returning to background levels (0.2 μg/L). These levels have not been shown to have effects on fish populations, although there are relatively few studies in this area, especially for chronic exposure. Observed levels in both lakes, however, approach the *Daphnia* 48-hour LC_{50}, suggesting that aquatic organisms in these systems are being impacted. Further study is needed in order to completely define the toxicological risks to indigenous species.

Microcystin concentrations were always higher in the highly eutrophic lake (Silver Lake) than at the control site (Casey Lake). There were, however, no significant relationships between microcystin concentrations in lake water or cell lysate and chlorophyll *a*, total phosphorus or relative cyanobacterial abundance. This result is puzzling, and contradicts at least one study in which microcystin concentrations were correlated with phosphate, although the investigated phosphorus concentrations were much lower than observed in these lakes. Future studies should elucidate the species composition and toxin profiles of cells from the two lakes to provide more information on the potential risks to humans and wildlife, and on the relationship between nutrients and toxin profiles.

Impacts of Research

The implications of this research for potential toxicological risks to aquatic organisms, and ultimately the health of lake ecosystems will be of great benefit in discussions pertaining to the regulation of non point source pollution, not only in Iowa lakes but also in all lakes potentially threatened by harmful algal blooms. Further research is needed to understand the relationship between toxin concentrations and nutrient profiles in eutrophic lakes with seasonal cyanobacterial populations. The results of this study may also indicate the need to consider the need for and to develop novel non-conventional mitigation actions for impacted lakes. Reduction in sources of nutrients to Iowa lakes will surely result in better water quality. Potassium (K) levels should also be considered, however, because potassium has been shown to suppress the growth of *Microcystis* (Parker et al 1997) and may therefore be a novel means of control of toxic cyanobacterial blooms.

References Cited

Bachman, R.W., T.A. Hoyman, L.K. Hatch and B.P. Hutchins. 1994. A Classification of Iowa's Lakes for Restoration. Technical Report. Department of Animal Ecology, Iowa State University.

Beveridge, M.C.M., D.J. Baird, S.M. Rahmatullah, L.A. Lawton, K.A. Beattie and G.A. Codd. 1993. Grazing rates on toxic and non-toxic strains of cyanobacteria by *Hypophthalmicthys molitrix* and *Oreochromis niloticus*. Journal of Fish Biology 43:901-907.

Boney, A.D. 1975. Phytoplankton. Edward Arnold, London.

Bourne, D.G., G.J. Jones, R.L. Blakeley, A. Jones, A.P. Negri and P. Riddles. 1996. Enzymatic pathway for the bacterial degradation of the cyanobacterial cyclic peptide toxin microcystin LR. Applied and Environmental Microbiology 62:4086-4094.

Bury, N.R., F.B. Eddy and G.A. Codd. 1995. The effects of the cyanobacterium *Microcystis aeruginosa*, the cyanobacterial hepatotoxin microcystin-LR, and ammonia on growth rate and ionic regulation of brown trout. Journal of Fish Biology 46:1042-1054.

Clesceri, L.S., A.E. Greenberg and A.D. Eaton (eds). 1998. Standard Methods for the Examination of Water and Wastewater, 20th Edition. American Public Health Association, Washington, D.C.

Craig, M., H.A. Luu, T.L. McCready, D. Williams, R.J. Andersen and C.F.B. Holmes. 1996. Molecular mechanisms underlying the interaction of motuporin and microcystins with type-1 and type-2A protein phosphatases. Biochemistry and Cell Biology 74:569-578.

Jochimsen, E.M., W.W. Carmichael, J. An, D.M. Cardo, S.T. Cookson, C. Holmes, M. Antunes, D. Filho, T. Lyra, V. Barreto, S. Azevedo and W.R. Jarvis. 1998. Liver failure and death after exposure to microcystins at a hemodialysis center in Brazil. New England Journal of Medicine 338:873-878.

Jungmann, D. and J. Benndorf. 1994. Toxicity to *Daphnia* of a compound extracted from laboratory and natural *Microcystis* spp., and the role of microcystins. Freshwater Biology 32:13-20.

Keshavanath, P., M.C.M. Beveridge, D.J. Baird. L.A. Lawton, A. Nimmo and G.A. Codd. 1994. The functional grazing response of a phytoplanktivorous fish *Oreochromis niloticus* to mixtures of toxic and non-toxic strains of the cyanobacterium *Microcystis aeruginosa*. Journal of Fish Biology 45:123-129.

Kotak, B.G., R.W. Zurawell, E.E. Prepas and C.F.B. Holmes. 1996. Microcystin-LR concentration in aquatic food web compartments from lakes of varying trophic status. Canadian Journal of Fisheries and Aquatic Science 53:1974-1985.

Lam, A., P.M. Fedorak and E.E. Prepas. 1995. Biotransformation of the cyanobacterial hepatotoxin microcystin-LR, as determined by HPLC and protein phosphatase bioassay. Environmental Science and Technology 29:242-246.

Lambert, T.W., M.P. Boland, C.F.B. Holmes and S.E. Hrudey. 1994. Quantitation of the microcystin hepatotoxins in water at environmentally relevant concentrations with the protein phosphatase bioassay. Environmental Science and Technology 28:753-755.

Lin, J.R. and F.S. Chu. 1994. Kinetics of distribution of microcystin-LR in serum and liver cytosol of mice: an immunochemical analysis. Journal of Agricultural and Food Chemistry 42:1035-1040.

Liu, B.H., F.Y. Yu and F.S. Chu. 1996. Anti-idiotype and anti-anti-idiotype antibodies generated from polyclonal antibodies against microcystin-LR. Journal of Agricultural and Food Chemistry 44:4037-4042.

McDermott, C.M., R. Feola and J. Plude. 1995. Detection of cyanobacterial toxins (microcystins) in waters of northeastern Wisconsin by a new immunoassay technique. Toxicon 33:1433-1442.

Osterhaus, L. 1999. Phytoplankton Species and Composition of Two Iowa Lakes. Technical Report. Environmental Programs, University of Northern Iowa.

Parker, D.L., H.D. Kumar, L.C. Rai and J.B. Singh. 1997. Potassium salts inhibit growth of the cyanobacteria *Microcystis* spp. in pond water and defined media: implications for control of microcystin-producing aquatic blooms. Applied and Environmental Microbiology 63:2324-2329.

Pouria, S. A. de Andrade, J. Barbosa, R.L. Cavalcanti, V.T.S. Barreto, C.J. Ward, W. Presier, G.K. Poon, G.H. Neild and G.A. Codd. 1998. Fatal microcystin intoxication in haemodialysis unit in Caruaru, Brazil. The Lancet 352:21-26.

Prepas, E.E., B.G. Kotak, L.M. Campbell, J.C. Evans, S.E. Hrudey and C.F.B. Holmes. 1997. Accumulation and elimination of cyanobacterial hepatotoxins by the freshwater clam *Anodonta grandis simpsoniana*. Canadian Journal of Fisheries and Aquatic Sciences 54:41-46.

Rapala, J., K. Sivonen, C. Lyra and S.I. Niemela. 1997. Variation of microcystins, cyanobacterial hepatotoxins, in *Anabaena* spp. as a function of growth stimuli. Applied and Environmental Microbiology 63:2206-2212.

Reinikainen, M., M. Ketola and M. Walls. 1994. Effects of the concentrations of toxic *Microcystis aeruginosa* and an alternative food on the survival of *Daphnia pulex*. Limnology and Oceanography 39:424-432.

Runnegar, M., N. Berndt, S.M. Kong, E.Y.C. Lee and L. Zhang. 1995. In vivo and in vitro binding of microcystin to protein phosphatases 1 and 2A. Biochemial and Biophysical Research Communications 216:162-169.

Sahin, A., F.G. Tencalla, D.R. Dietrich, K. Mez and H. Naegeli. 1995. Enzymatic analysis of liver samples from rainbow trout for diagnosis of blue-green algae-induced toxicosis. American Journal of Veterinary Research 56:1110-1115.

Toivola, D.M., J.E. Eriksson and D.L. Brautigan. 1994. Identification of protein phosphatase 2A as the primary target for microcystin-LR in rat liver homogenates. FEBS Letters 344:175-180.

Tsuji, K., S. Nalto, F. Kondo, N. Ishikawa, M.F. Watanabe, M. Suzuki and K.I. Harada. 1994. Stability of microcystins from cyanobacteria: effect of light on decomposition and isomerization. Environmental Science and Technology 28:173-177.

Ward, C.J., K.A. Beattie, E.Y.C. Lee and G.A. Codd. 1997. Colorimetric protein phosphatase inhibition assay of laboratory strains and natural blooms of cyanobacteria: comparisons with high-performance liquid chromatographic analysis for microcystins. FEMS Microbiology Letters 153:465-473.

Information Transfer Program

The results of the proposed research will be of interest to resource managers and environmental scientists concerned with water quality. This work was presented at the Agriculture and the Environment: State and Federal Water Initiatives workshop at Iowa State University in March. Additionally, in conjunction with the UNI Lake Water Quality Study, we have developed working relationships with individuals from the Iowa Department of Natural Resources, the Delaware and Black Hawk County Conservation Boards, the Natural Resources Conservation Service, and citizens groups concerned with water quality issues in Silver Lake and Lake Delhi. Representatives of these groups are members of an advisory board associated with the UNI Lake Water Quality Study. The results of this research will be transmitted to resource managers and other interested parties as part of the next advisory board meeting. I have also been in contact with Mr. Bud Cann of the New Jersey Department of Environmental Protection Lakes Program about this research and the potential significance of cyanobacterial blooms resulting from nutrient enrichments, so the outcomes of this research will be also be disseminated to interested resource managers outside of the state of Iowa. The scientific results of and conclusions from this study will also be communicated to environmental scientists through a manuscript which is in preparation for publication in the peer reviewed literature.

Basic Information

Title:	Effect of liquid swine manure application to water quality from soil infiltration areas and wetlands
Project Number:	B-06
Start Date:	3/1/2000
End Date:	2/28/2001
Research Category:	Not Applicable
Focus Category:	Water Quantity, Waste Water, Water Quality
Descriptors:	Manure, animal waste, subsurface drainage, bacteria
Lead Institute:	Iowa State Water Resources Research Institute
Principal Investigators:	Jeffery Lorimor, Larry J. Halverson

Publication

Problem and Research Objectives

This research is a laboratory scale project conducted on small field plots and lysimeters, both in the laboratory and in the field. The overall objective of this project is to understand the soil microbial and chemical processes occurring within infiltration areas and wetlands used to treat liquid swine manure to enable effluents to be of sufficient quality to be discharged to Iowa's water bodies safely. (Discharges from animal facilities are not allowed now, but may become an option in the future if effective treatment systems can be developed). Rather than answering the question "what's happening?" the proposed project will also answer the question "why is it happening in the proposed treatment system?" Instead of determining whether bacteria are present in the soil filtrate and wetland effluent, we will determine whether the source of that bacteria is from swine manure or from naturally occurring activities in the soil-water system. *This is a request for second year funding to continue the project.*

Methods, Procedures, and Facilities

A set of 18 (9 pairs) of 210L plastic containers located in the field and are being used for the study. In each set of two containers, the first is designed for soil infiltration, the second just below first set serve as wetlands. They are designed so that flows in and out of each container can be monitored and sampled for nitrogen, phosphorus, and bacteria. This set of containers is subject to climatic and hydrologic events occurring throughout the year.

A second set of undisturbed soil cores have been obtained by driving 20 cm diameter steel cylinders into the soil. This set of cores is inside Dr. Lorimor's laboratory at ISU where they are isolated from outside daily climatic and hydrologic events

To determine whether the bacteria from the manure are actually transported through the soil columns, genetically marked bacteria have been isolated to use as tracers. A genetically marked psuedomonad or a bacillus species from the manure system were isolated. The genetic marker used is a green fluorescent protein which provides a readily visible marker since it makes the bacteria turn bright green color. The genetically marked bacteria were introduced into the manure and maintained for some period of time (2 weeks) to verify that the marker has not decreased their ability to survive in the manure. The manure with the marked bacteria were applied to the soil.

The primary independent variables being investigated in the outdoor system are:

Manure –applied every two weeks at full rate based on nitrogen utilization
Manure – applied every two weeks at ¾ N rate
Water only – applied every two weeks based on soil moisture holding capacity

Treatments in the indoor columns are designed to determine if time and desiccation due to drying soils affect bacteria survival and transport:

Manure – one application only to all columns except the checks at 5000 gallons/ac,

Treatment 1 – one application of 2 inches of water at 4 days after manure application
again at 8 days, and again at 16 days
Treatment 2 one application of 2 inches of water at 8 days, and again at 16 days
Treatment 3 one application of 2 inches of water at 16 days

Research identifies macropores as one of the primary pathways for bacterial movement. Three tillage treatments designed to destroy macropores superimposed on the above water treatments in the laboratory experiment will help delineate the contribution macropores play in bacterial movement. The treatments are 1) notill manure broadcast, 2) tillage ahead of broadcasting manure, and 3) manure injection. The effluent will be monitored for the marked bacteria. At the end of the experiment, the soil columns will be sampled at the top, middle, and bottom to determine the number of genetically marked and naturally occurring bacteria in the soil.

Conclusions

Since we have just begun the first year of this study, no major conclusions have been reached.

Basic Information

Title:	Occurrence and formation of nitrosamines in drinking water distribution systems
Project Number:	B-07
Start Date:	3/1/2000
End Date:	2/28/2001
Research Category:	Not Applicable
Focus Category:	Water Quality, Toxic Substances, Water Supply
Descriptors:	Water chemistry, water quality, water treatment, disinfection, and chlorination
Lead Institute:	Iowa State Water Resources Research Institute
Principal Investigators:	Richard L. Valentine

Publication

Research Background.

Many nitrosamines, especially N-dimethylnitrosamine (NDMA), are potent carcinogens. A number of past studies and current observations support the hypothesis that nitrosamine (NA) occurrence and formation could be an especially important problem in some Midwestern drinking water distribution systems. While the exact conditions and mechanisms leading to nitrosamine formation in the environment are not well understood, it is known that they are formed by reaction of nitrite with certain organic nitrogen containing (amine) compounds.

These precursors to NA formation are ubiquitous in many Midwest drinking water sources or can actually be formed in distribution systems thus possibly making these supplies susceptible to nitrosamine formation. Additionally, recent observation in California suggests that NDMA formation may be related to disinfection practices, suggesting that at least this nitrosamine should also be considered a "new" disinfection by-product.

Little is known, however, about the occurrence and formation potential of nitrosamines in Midwestern drinking water distribution systems. To date, no systematic studies have considered the potential for nitrosamine formation in distribution systems and possible spatial and temporal variability. Research is needed to characterize the extent of this potential problem, and to determine how water quality, treatment, and distribution system characteristics influence it. The relationship of nitrosamine formation and occurrence to disinfection and in-system processes, especially those influenced by the pipe-water interface, needs to be ascertained. A fundamental understanding of the reaction kinetics and mechanisms would also be of great benefit in developing strategies to minimize exposure to these contaminants.

Objective(s) of the Research Project:

Based on the ascertained research needs, the following specific objectives with rationale were formulated for this research study:

1. Assess the spatial and temporal occurrence of selected nitrosamines, especially NDMA, in several midwestern water distribution systems.

2. Conduct laboratory based studies to examine mechanisms and fundamental factors influencing nitrosamine formation especially disinfection, and the presence of pipe and attached deposit material.

3. Relate field and laboratory findings to provide an assessment of the significance of nitrosamine occurrence and formation as a consequent of source water quality, water treatment and distribution, and to propose strategies to minimize occurrence and formation.

Progress Summary/Accomplishments:

Work has progressed in several areas. These include 1) developing NDMA analysis methods and 2) investigating the hypothesis that NDMA is a water treatment by-product. We have developed an analytical method for NDMA appropriate for analysis of relatively high concentrations. This method first involves extraction of the NDMA using 200 mg/L of an Ambersorb 572 resin followed by extraction using 1 ml of methylene chlorine. Qualitative compound identification is done using GC-Low Resolution MS based on retention time and relative abundance of three characteristic masses (m/z). Quantitative analysis uses d6-NDMA internal-standard techniques with a single characteristic m/z. The MDL for this method is 200 ng/L.

It is well established that NDMA can be formed by reaction of certain organic nitrogen containing precursors with nitrite (conventional nitrosation pathway). We initiated laboratory studies to investigate the hypothesis that a new NDMA formation pathway exists that involves a reaction of nitrogenous precursors with chlorine or chloramine disinfectants. In otherwords, NDMA is novel disinfectant by-product. Our studies show that monochloramine, a common disinfectant used in distribution system does indeed react with dimethylamine (a model organic nitrogen containing precursor) to produce NDMA. We conclude that conventional nitrosation and this novel pathway may be important reactions leading to NDMA formation. The latter would account for its formation as a consequence of water treatment. Additional work investigated the kinetics of the reaction and utilized isotope methodology to prove that the nitrogen from monochloramine is the source of the nitro group of NDMA when formed by this new pathway.

Future Activities:

We are continuing our laboratory studies to better characterize NDMA formation reactions especially the reaction of monochloramine with various nitrogenous compounds. We will purchase a large volume injector to improve our NDMA analytical capability, hopefully allowing us to reach an MDL of approximately 2 ng/L. We will also initiate a survey on the occurrence of NDMA in drinking waster. The scope of this work will be expanded to include additional utilities in the US and Canada through collaboration with the Metropolitan Water District of Southern California, Orange County Water District of Southern California, and the Department of Civil and Environmental Engineering of the University of Waterloo (Canada).

Additional Support.

The PI was recently awarded a $400,000 grant from the Water Environment Federation and the American Water Works Association Research Foundation to study factors governing the formation of NDMA and occurrence in drinking and wastewater. The proposal for this grant included results obtained using ISWRRI support that were critical to its successful selection. This new grant, which begins in January 2001, effectively leverages the continuing ISWRRI support, which is requested and should be considered as additional support generated by ISWRRI.

The WEF-AWWARF study is a partnership with the Metropolitan Water District of Southern California, Orange County Water District of Southern California, and the Department of Civil and Environmental Engineering of the University of Waterloo (Canada). The scope of the work is considerably larger and more involved in the ISWRRI proposal, especially in regards to conducting an extensive survey of occurrence.

Basic Information

Title:	Treatment of nitrate-contaminated groundwater using Fe(0) and autotrophic denitrifiers
Project Number:	G-01
Start Date:	9/1/1998
End Date:	8/28/2000
Research Category:	Not Applicable
Focus Category:	Nitrate Contamination, Groundwater, Methods
Descriptors:	Nitrates, groundwater, contamination
Lead Institute:	Iowa State Water Resources Research Institute
Principal Investigators:	Pedro J. Alvarez

Publication

1. Ginner J. L., Pedro J. Alvarez, Michael J. Alowitz, Sharon L. Smith, and Michelle M. Scherer (2001). Mass Transport and Temperature Effects on the Kinetics of Nitrate and Nitrite Reduction by Iron Metal. In preparation for Water Research.
2. Dejournett T. and P.J.J. Alvarez (1999) Combined microbial-Fe(0) system to remove nitrate from contaminated groundwater. Bioremediation 4:149-154.
3. Scherer, M.M., J. Ginner, P.J.J. Alvarez, and K. Johnson (2000). Contaminant remediation by iron metal: shifting kinetic regimes. Proc. Hazardous Waste Research 2000 Conference. Denver, CO. May 23-25, 2000.
4. Dejournett T. and P.J.J. Alvarez* (1999) Combined Microbial-Fe(0) System to Treat Nitrate-Contaminated Groundwater; In: B.C. Alleman and A. L. Leeson (eds.), In Situ and Onsite Bioremediation, Battelle Press, 5(4): 79-84.
5. Ginner G., S. Therkelsen, M. Scherer, and P.J.J. Alvarez (1999). Nitrate reduction by iron metal: the rate limiting step. Proc. 14th HSRC Conference on the Hazardous Waste Remediation, Saint Louis, MO, May 19-21, 1999.

The general goal of this project was to develop a new and efficient method to remove nitrate from contaminated groundwater. This method is based on combining a novel chemical process (reductive treatment with Fe(0)) with a promising bioremediation approach (*in situ* reactive zones). Laboratory experiments that address critical knowledge gaps were performed during two years to remove nitrate under various geochemical and hydraulic conditions. Specific objectives include:

1) Delineate the applicability and limitations of biologically-active semipermeable Fe(0) barriers to intercept and remove nitrate and/or nitrite from groundwater plumes, and to obtain basic criteria for the design and operation of biologically active Fe(0) barriers.

2) Determine how environmental factors and substrate interactions affect the efficiency of bioaugmented Fe(0) barriers to attenuate nitrate migration under various hydraulic regimes. The following variables were considered: (1) the organic carbon content of the aquifer material, which represents a potential electron donor pool to sustain denitrification; (2) the presence of aluminosilicate minerals, which may buffer the Fe(0)-corrosion-induced increase in pH that inhibits microorganisms; and (3) the limits of hydraulic loadings that can be handled by a biologically-active Fe(0) barrier to intercept and treat nitrate plumes.

3) Determine whether the rate of nitrate and nitrite reduction by iron metal is controlled by mass transport to the iron surface or by chemical reaction at the iron surface.

4) Characterize the effect of temperature on the rate of nitrate removal by Fe(0), cells, and combined treatment systems.

HYPOTHESES

Fe(0) can stimulate microbial denitrification in carbon-limited aquifers not only by rapidly inducing anoxic conditions during its aerobic corrosion, but also by donating electrons to the respiratory chain during its anaerobic corrosion (via water-derived cathodic H_2) (Figure 1). Bacteria, in turn, can enhance abiotic nitrate reduction by removing the passivating H_2 layer from the Fe(0) surface to enhance surface corrosion of Fe(0), and thus, the flow of electrons (i.e., cathodic depolarization). Thus, combining Fe(0) with hydrogenotrophic denitrifiers will synergistically increase the nitrate removal efficiency in aquifers where denitrification is limited by the availability of suitable electron donors. This beneicial effect can be enhanced by adding montmorillonite clay to buffer against the corrosion-induced pH increase. This will allow increased microbial participation and will also enhance Fe(0) corrosion

Regarding removal kinetics, nitrate reduction by iron metal will be surface-reaction controlled and the rate if nitrate transport to the iron metal surface should not be rate limiting. On the other hand, nitrite reacts much faster with iron metal and mass transfer to the iron surface will influence its reduction by iron metal. Finally, denitrifying bacteria will lower the activation energy and allow the reduction of nitrate and nitrite to proceed at a faster rate.

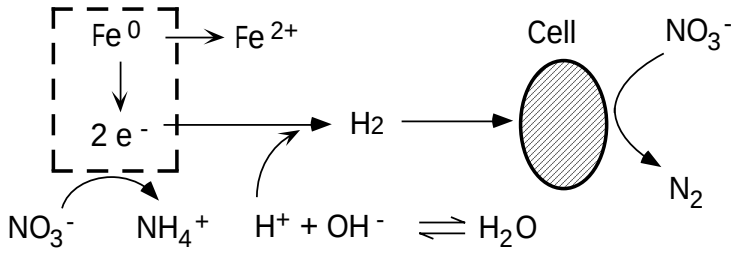

Figure 1. Concept of Fe(0)-Supported Denitrification

MATERIALS AND METHODS

Aquifer microcosms were prepared in duplicate using 250-mL serum bottles capped with Mininert valves. All microcosms were amended with 90 grams of either top garden soil (2.5% org-C) or sand (0.1% org-C) plus 100 mL of bicarbonate-buffered mineral medium containing inorganic nutrients and 30 mg/L NO_3^--N. The medium recipe is described elsewhere (Till et al., 1998). Some microcosms were amended with montmorillonite clay. These contained 80 grams of low-carbon soil and 10 grams of montmorillonite (Fisher Scientific). Biological and abiotic transformations were studied separately and interactively by including or excluding Fe(0) (10g Fisher Fe-filings, 0.1410 m^2/g) and denitrifying hydrogenotrophs (10 mL of *Paracoccus denitrificans*, ATTC# 17741, OD_{600}=0.006). Abiotic removal was assessed per NH_4^+ accumulation (Till et al., 1998), and biological denitrification was quantified per N_2O accumulation in acetylene-blocked microcosms (Yoshinari and Knowles, 1976).

The feasibility of bioaugmenting Fe(0) in sandy soil was also investigated in continuous-flow columns. Glass columns (26.5 cm long, 2.5 cm diameter) were packed with a mixture of sand and Fe(0) filings (15% by weight). One column was autoclaved to discourage growth of indigenous microbes, while the other was seeded with *P. denitrificans*. Mineral medium containing 33 mg/L NO_3^--N was pumped through the columns in an upflow mode using a Masterflex® (Barrington, IL) 7523-30 peristaltic pump with a 519-15 pump head. The flowrate was varied from 0.02 mL/min to 0.16 mL/min (i.e., hydraulic retention time (HRT) = 0.25 to 2 days). The influent reservoirs were 5000-mL Pyrex jars topped with Teflon®-lined delivery caps. These reservoirs were continuously purged with an N_2/CO_2 (80:20 v/v) gas mixture using tubing with a stone diffuser. At the end of the 152-day experiment, samples were taken from the soil/Fe(0) matrix and examined under a scanning electron microscope.

Electrochemical experiments were conducted to determine whether mass transport to the iron surface or the chemical reaction at the iron surface controls the overall reduction rate of nitrate and nitrite by Fe(0). These experiments were conducted in a custom three-electrode glass cell apparatus equipped with a rotating disk electrode as described in Jennifer Ginner's thesis (attached). Batch experiments were also used to determine the effect of temperature on the rate of nitrate and nitrite reduction by iron metal and the effect that microbes have on the activation energy. In all cases, nitrate and nitrite were analyzed using a Dionex BioLC ion chromatograph, and ammonium was measured with a Dionex DX-100 ion chromatograph. Additional experimental details can be found in the Maters theses included in the appendix.

RESULTS AND DISCUSSION

Semi-permeable reactive Fe(0) barriers are particularly attractive for groundwater remediation in that they conserve energy and water, and through long-term low operating and maintenance costs, have the potential to be considerably less costly than conventional cleanup methods. Early studies of Fe(0) barriers found little microbial contribution to contaminant degradation, and research has focused primarily on abiotic processes. Nevertheless, the potential for microorganisms to enhance reductive treatment with Fe(0) has been demonstrated in recent laboratory experiments (Till *et al.*, 1998; Weathers *et al*., 1997). This work corroborates that microbial utilization of cathodic hydrogen is a critical link between biogeochemical interactions and enhanced contaminant removal.

Batch Aquifer Microcosms. Microcosms prepared with high-carbon (2.5%) top soil removed nitrate relatively fast (ca. 30 mg/L as N within 4 days), regardless of whether they were amended with Fe(0), *P. denitrificans*, both, or none. Apparently, indigenous microorganisms utilized naturally occurring organic matter as electron donors to denitrify. Thus, neither Fe(0) nor bacterial amendment enhanced NO_3^- removal in high-carbon top soil. In contrast, adding Fe(0) to low-carbon (0.1%) sandy soil had a beneficial effect compared to control microcosms without Fe(0). These controls exhibited no nitrate removal, possibly due to a low concentration of suitable electron donors in the sandy soil. Adding Fe(0) supplemented the electron donor pool and enhanced nitrate removal below the MCL (10 mg/L as N) within 20 days (Figure 2).
Adding *P. denitrificans* to Fe(0)-amended, low-carbon microcosms did not enhance nitrate removal. These microcosms experienced a large increase in pH (i.e., pH>10 after 25 days) due to Fe(0) corrosion (equation 1). Such high pH levels are known to inhibit microbial denitrification (Till et al., 1998). Therefore, abiotic nitrate reduction by Fe(0) outcompeted the biological denitrification pathway. This notion is supported by the stoichiometric reduction of nitrate to ammonium, which is the end product of the abiotic reaction, and by the absence of (microbially-produced) N_2O in acetylene-blocked microcosms (data not shown). This indicates that pH control may be important to sustain Fe(0)-based denitrification.

Montmorillonite clay has been reported to buffer against the corrosion-induced pH increase in Fe(0) systems. This is accomplished through a series of dissolution and proton-generating reactions at the Fe(0) surface (Powell and Puls, 1997). Thus, the presence of such acidic aluminosilicate minerals may improve the reactivity of Fe(0) barriers. This is illustrated in Figure 3, which depicts the ability of montmorillonite to enhance nitrate removal in Fe(0)-amended microcosms. These microcosms were sterilized to isolate the effect of montmorillonite on iron reactivity. Interestingly, adding montmorillonite (11% by weight) also prevented the accumulation of the more toxic intermediate, nitrite. This was attributed to enhanced Fe(0) reactivity due to a lower pH at the Fe(0) surface. Enhanced Fe(0) reactivity in montmorillonite-amended microcosms was also indicated by higher H_2 evolution (data not shown).

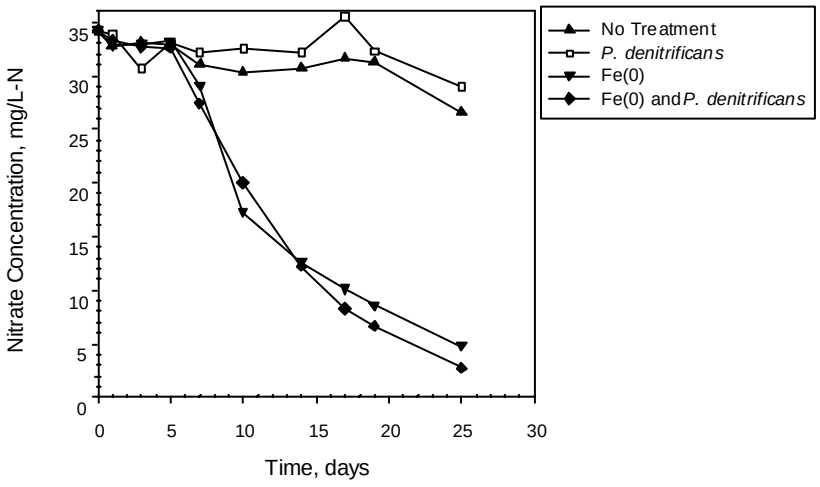

FIGURE 2: Nitrate removal in low-carbon (0.1%) aquifer microcosms.

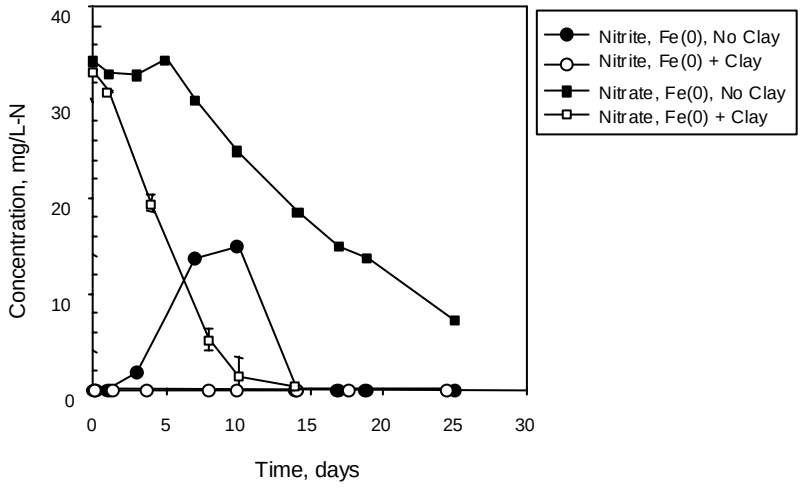

FIGURE 3: Effect of montmorillonite clay (11% by weight) on abiotic nitrate removal by Fe(0) and transient accumulation of nitrite. Data corresponds to microcosms that were poisoned with 300mg/L $HgCl_2$. Error bars depict one standard deviation from the mean of triplicate microcosms.

A five-day lag period was observed in Fe(0)-amended microcosms (Figures 2 and 3). During this period, little nitrate removal was observed. The reason for this lag period is unknown, although the fact that it also occurred in sterile (poisoned) microcosms suggests that it was related to iron chemistry rather than to microbial activity. Some researchers suggest that H_2 adsorbed to the Fe(0) surface, rather than the Fe(0) itself, may be responsible for contaminant reduction (Grittini, et al., 1995; Schrier and Reinhard, 1995). According to this untested hypothesis, Fe(0) may act as a catalyst, activating H_2 in a manner similar to metals such as palladium. Perhaps the lag period reflects the time required to accumulate enough H_2 at the Fe(0) surface to facilitate the reaction. Alternatively, the Fe(0) used in this experiment was not acid washed, which raises the possibly that there was an oxide layer acting as a barrier to electron transfer (Scherer et al., 1998). Thus, the lag period could also reflect the time required to "activate" this layer by either reducing it with electrons from the inner core of the iron, or by building up aqueous concentrations of ferrous iron to form a reactive oxide. Interestingly, adding montmorillonite eliminated this lag period (Figure 3), which reiterates the potential for acidic minerals to enhance the reactivity of iron barriers.

Column Studies. The influent solution to both columns had a pH of about 7.0 units and a dissolved oxygen (DO) concentration of about 1 mg/L. The effluent pH was about 8.0 units for both columns, and no DO was detected in the effluents (DO < 0.1 mg/L). Figure 4 depicts effluent nitrate concentrations for different hydraulic retention times (HRT). Nitrate removal efficiencies were similar for bioaugmented and unamended columns. Decreasing the HRT had an adverse effect on nitrate removal efficiency. By day 123, at an HRT of 0.25 days, the nitrate concentration in both columns increased to 25 mg/L NO_3^--N. This corresponds to relatively low (17%) removal efficiency. Yet, increasing the HRT back to 1.0 day decreased the effluent nitrate concentration below 10 mg/L (as N) for both columns (73% removal efficiency). This indicates that the loss of nitrate removal capacity was due to hydraulic overloading, which results in HRTs that are too short for efficient nitrate removal, rather than to exhaustion of Fe(0) reactivity over time. The typically slow flow velocity of groundwater would ensure long retention times conducive to high removal efficiencies.

Nitrite is a toxic intermediate of nitrate reduction by both the abiotic and biological pathways. Figure 5 depicts the effluent nitrite concentration in this same experiment. Effluent nitrite concentrations from the unamended column increased to as high as 7 mg/L NO_2^--N early in the study, while nitrite concentrations in the effluent of the bioaugmented column generally remained below the MCL (1 mg/L NO_2^--N). This was attributed to microbial denitrification of nitrite to N_2. As the columns acclimated over time, nitrite was eliminated from the effluent of both columns. Acclimation of the autoclaved column was attributed to the fact that microbial activity was not completely eliminated, reflecting the difficulty to successfully sterilize soil and to keep such column systems sterile over extended periods of time.

The effluent ammonium concentrations for both columns followed similar trends, peaking at about 30 mg/L NH_3-N after seven weeks when the HRT was 1.0 day. Ammonium concentrations decreased subsequently in both columns below 10 mg/L NH_3-N, suggesting an increase in nitrate removal by microbial denitrification.

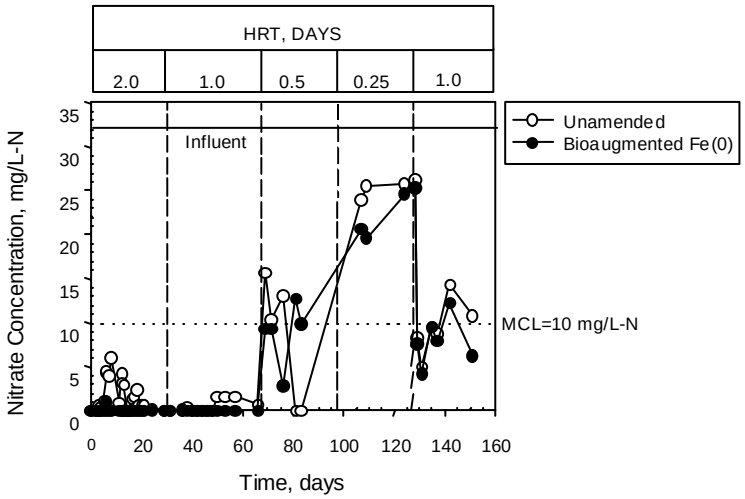

FIGURE 4. Effect of hydraulic retention time (HRT) on the effluent nitrate concentration from aquifer columns.

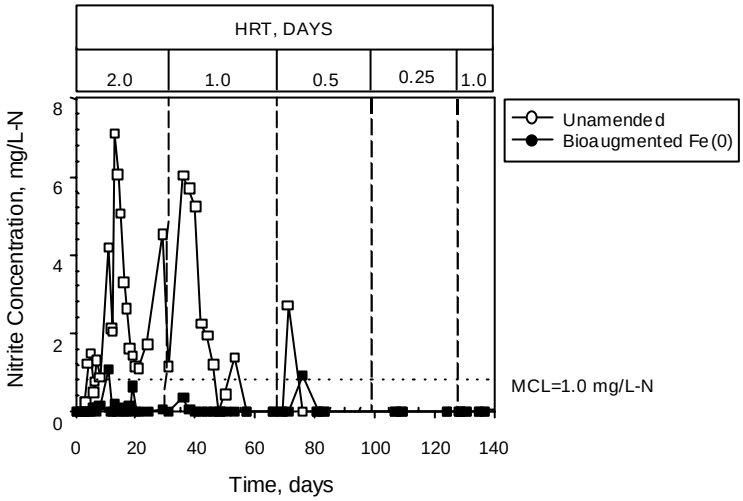

FIGURE 5. Effluent nitrite concentration from continuous flow columns.

Soil and Fe(0) filings from the columns were analyzed at the end of the experiment using scanning electron microscopy. Bacteria were found to selectively colonize the Fe(0) surfaces (over soil grains) in both columns. This suggests that indigenous denitrifiers may colonize Fe(0) barriers to exploit cathodic depolarization as a metabolic niche. The selective colonization of Fe(0) surfaces would facilitate microbial uptake of relatively insoluble cathodic H_2.

In summary, biologically-active Fe(0) barriers hold great promise for treating groundwater contaminated with nitrate, and should also be considered to treat other redox-sensitive priority pollutants. Bioaugmentation of the barrier matrix with autotrophic denitrifiers can shorten the acclimation period required for indigenous bacteria to colonize the Fe(0) surface. Alternatively, an indigenous hydrogenotrophic consortium is likely to eventually develop around an H_2-producing Fe(0) barrier. Once microbial populations are established, the bacteria may enhance the treatment process by reducing the amount of nitrite accumulating as an intermediate of abiotic nitrate reduction, and improve Fe(0) corrosion kinetics by removing the passivating H_2 layer from the Fe(0) surface. Thus, appropriate bacteria can enhance both the rate and extent of transformation and yield a more favorable end product distribution.

Effect of mass transfer on kinetics of nitrate and nitrite reduction by iron metal.
Electrochemical experiments were conducted to determine whether mass transport to the iron surface or the chemical reaction at the iron surface controls the overall reduction rate of nitrate and nitrite by iron metal. An oxide-free rotating disk electrode (RDE) was used for this purpose. This instrument is described in Jennifer Ginner's thesis (Appendix B). Electrode rotation rate was found to have little effect on the rate of NO_3^- reduction at the oxide-free Fe^0 electrode, indicating that the rate of NO_3 reduction was limited by reaction at the Fe^0 surface (Figure 6). The rate of NO_2^- reduction, on the other hand, was strongly influenced by the electrode rotation rate, as shown in Figure 6 for four NO_2^- concentrations. Higher NO_2^- concentrations result in larger current densities over the entire range of rotation rates. The proportional increase in current density with NO_2^- concentration confirms that NO_2^- reduction at the Fe^0 RDE is a first-order process.

The lack of influence of electrode rotation rate on nitrate reduction rates suggest that the rate of nitrate reduction is controlled by the chemical reaction at the iron electrode surface. Under field conditions, the influence of mass transport may become more evident as the diffusion layer increases due to changes in mixing and the formation of oxides on the iron surface. The growth of the diffusion layer under field conditions may or may not change what is limiting the rate of nitrate removal by iron metal (Scherer et al., 1998). Comparison of nitrate reduction rates with mass transport rates estimated for an Fe(0) reactive barrier, however, suggest that under field conditions it is more likely that reaction will limit nitrate reduction rates (Scherer et al., 2001).

Nitrite reduction, on the other hand, is clearly influenced by mass transport to the iron electrode surface (Figure 7). Since mass transport rates at the electrode are much faster than those estimated for an Fe(0) reactive barrier, it is likely that some mass transport limitations will exist in field scale installations. This suggests that more efficient nitrite removal may be achieved in PRBs through better design of the flow through the barrier. If the flow of nitrite contaminated ground water was increased within the PRB, the reduction rate of nitrite would also increase. The increased flow through the iron wall can be achieved through better hydraulic designs (such

as funnel and gate systems). However, increasing the flow rate within the wall may result in insufficient contact time between the contaminated groundwater and the iron metal. It may be necessary to increase the thickness of the iron wall to ensure sufficient contact time if the groundwater flow velocity is significantly increased.

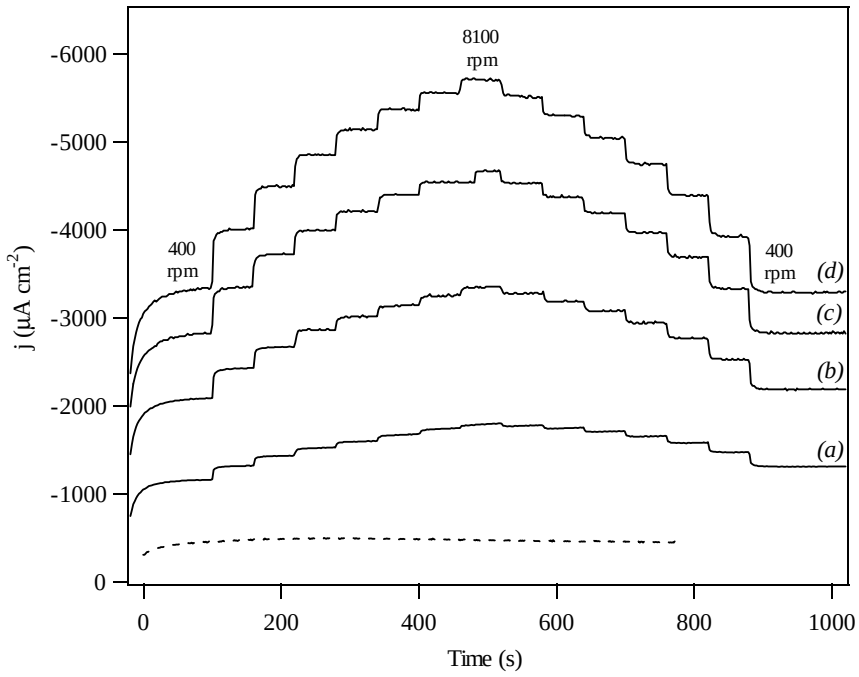

FIGURE 6. Time traces for constant potential reduction of NO_3^- (dashed line) and NO_2^- (solid lines) at an Fe^0 RDE with stepwise variation in rotation rate. Potential was held constant at –640 mV in a pH 8.4 borate buffer solution. Rotation rates for NO_2^- concentrations of (*a*) 0.03 M (*b*) 0.05 M (*c*) 0.08 M (*d*) 0.1 M NO_2^- varied from 400 to 8100 rpm. Rotation rates for 0.14 M NO_3^- were varied from 600 to 3600 rpm.

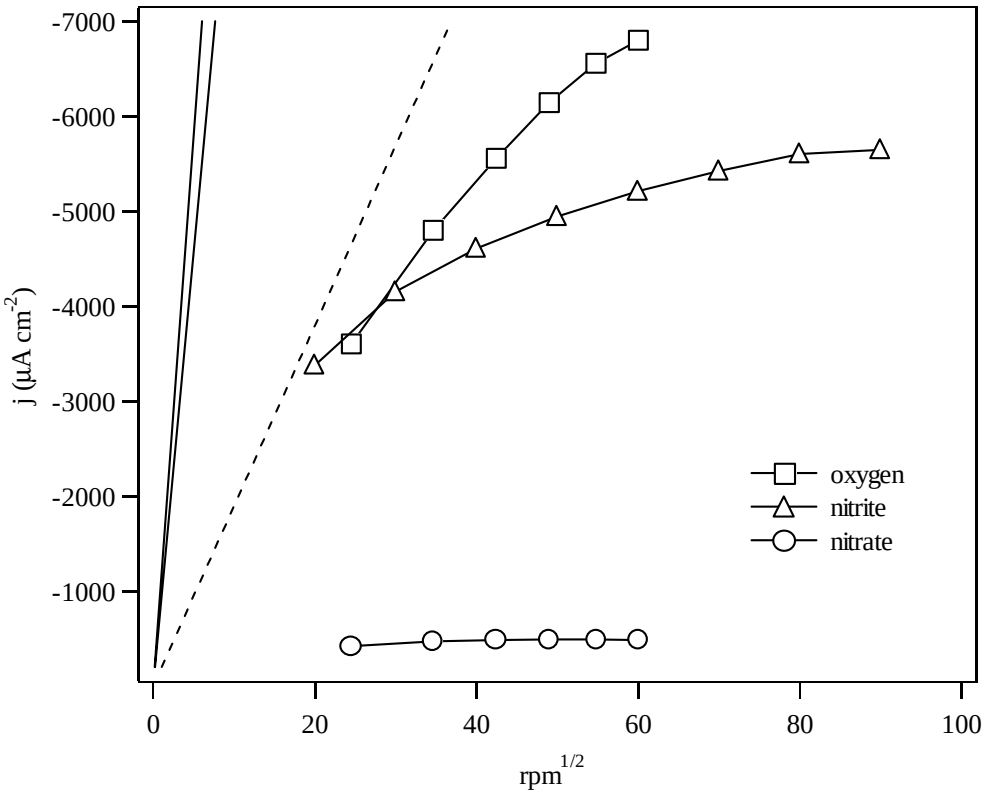

FIGURE 7. Effect of rotation rate on O_2, NO_3^- and NO_2^- current densities at an Fe^0 RDE. Steady-state current densities at –638 mV for oxygen-saturated pH 8.4 borate buffer (squares), 0.135 M NO_3^- (circles), 0.10 M NO_2^- (triangles), theoretical line for O_2 under mass transport control

Results showed also that the kinetics of nitrate reduction by iron metal is first-order with respect to amount of iron available to serve as a reductant (Figure 8). The strong influence of Fe availability on reduction rates suggests that the presence of multiple contaminants may inhibit individual contaminant reduction rates.

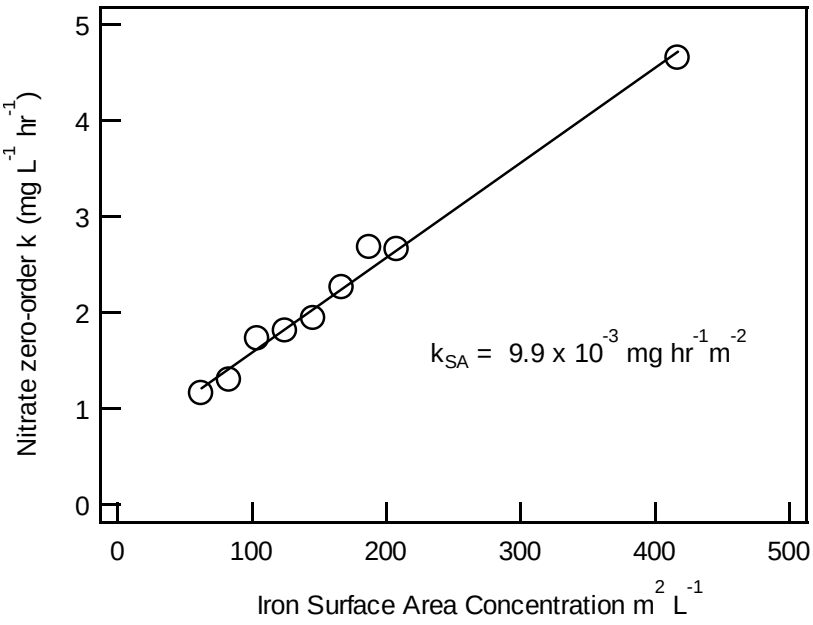

Fig. 8. Effect of Fe metal surface area concentration on kinetics of nitrate reduction. The linear increase in the zero-order rate coefficient suggest that the kinetics of nitrate reduction are first-order with respect to iron metal surface area concentration. The slope of the line provides a surface area normalized rate coefficient that is useful for predicting reduction rates at different iron loadings.

Effect of Temperature. We also investigated how temperature affects the removal rate of nitrate and nitrite. Temperature had a significant effect on the removal rate of both nitrate and nitrite by iron metal in batch systems (Table 1). The removal rate of nitrite was much faster than the removal rate of nitrate at all temperatures tested. Consistent with the observations in the RDE experiments described above, the activation energy for nitrate removal by iron metal in batch systems was 36.3 ± 9.08 kJ mol^{-1}, which is slightly indicative of surface-reaction control (Figure 9). The activation energy of nitrite removal by iron metal in batch system was 23.8 ± 3.95 kJ mol^{-1}, which is slightly indicative of mass transport control or mixed control. The batch temperature study indicated that nitrate removal by iron metal requires greater activation energy than nitrite removal.

These batch experiments also showed that cells could enhance nitrate-removal kinetics not only because they increase the flow of electrons through cathodic depolarization, but also because cells can lower the activation energy of the reaction. This leads to faster reaction rates, as illustrated in Figure 9. This is not surprising, since cells contain catalysts like enzymes that are known to decrease the activation energy and make the reaction go faster. These experiments also helped delineate the applicability of the iron-supported denitrification at different temperatures. The data showed that this process could work within the temperature range of 5 to 50 C.

TABLE 1. Effect of temperature and microbes on the rates of NO_3^- and NO_2^- reduction by granular Fe^0 in batch experiments. Batch reactors were amended with 7 g Master Builder iron filings (not acid washed) in buffered mineral medium containing either 0.7 mM NO_3 or NO_2. Biotic reactors were seeded with 20 mL of a stock culture of *Paracoccus denitrificans*. All batch reactors were incubated in the dark

Reactor Type	First-Order Rate Coefficient (hr^{-1})			
	5 °C	25 °C	35 °C	50 °C
Nitrite and Iron Metal	0.081 ± 0.007	0.140 ± 0.010	0.250 ± 0.012	0.334 ± 0.051
Nitrate and Iron Metal	0.011 ± 0.002	0.011 ± 0.001	0.020 ± 0.001	0.045 ± 0.002
Nitrate, Iron Metal and Microbes	0.025 ± 0.002	0.101 ± 0.007	0.146 ± 0.003	0.192 ± 0.018

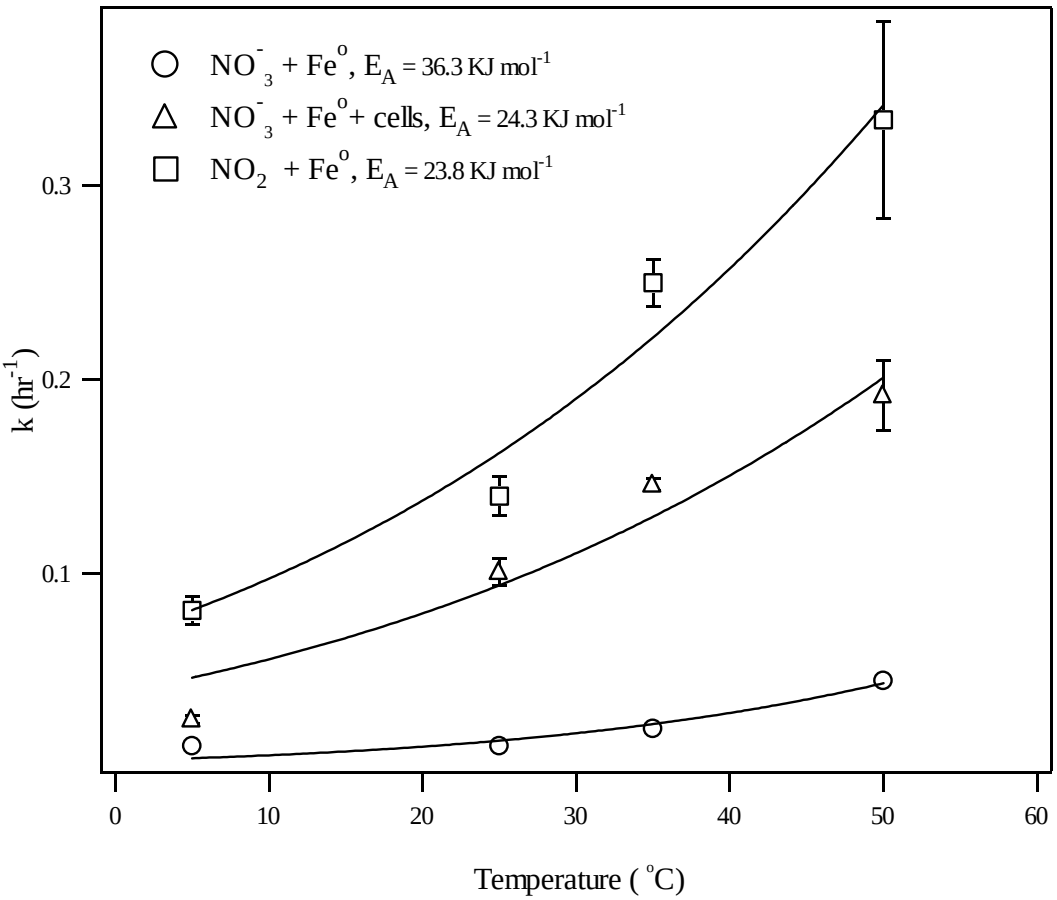

FIGURE 9. Effect of temperature and microbes on the activation energies of nitrate and nitrite reduction by granular Fe^0. Batch reactors were amended with 7 g Master Builder iron filings (not acid washed) in buffered mineral medium containing either 0.7 mM NO_3^- or NO_2^-. Biotic reactors were seeded with 20 mL of a stock culture of *Paracoccus denitrificans*. All batch reactors were incubated in the dark while continuously rotated.

CONCLUSIONS

Laboratory experiments showed that a combined biological-Fe(0) treatment approach holds great promise for treating nitrate-contaminated groundwater. Specific conclusions from the microcosms and aquifer column experiments (Todd Dejopurnett's thesis – Appendix A) include:

1. The addition of Fe(0) and/or hydrogenotrophic denitrifiers will be more beneficial for soil or aquifer material with a low carbon content. While the addition of Fe(0) was beneficial in low-carbon microcosms, the addition of *Paracoccus denitrificans* was not. This was believed to be due to either high pH associated with Fe(0) corrosion or the low density of the liquid inoculum. No Fe(0) treatment was required in the high-carbon soil microcosms. Apparently, indigenous heterotrophic denitrifiers were capable of rapidly removing all nitrate using the naturally occurring organic matter

.

2. Aluminosilicate minerals such as montmorillonite can enhance the treatment process by buffering against pH increase and enhancing Fe(0) corrosion. The enhanced removal kinetics were attributed to the additional protons generated by the montmorillonite. Montmorillonite addition also reduced the amount of nitrite produced as an intermediate in the reduction of nitrate to ammonium by Fe(0). This was thought to be associated with the lower pH.

3. The addition of *Paracoccus denitrificans* did not enhance the nitrate removal kinetics in the continuous-flow columns, but it did reduce the amount of nitrite eluted from the columns. Thus, it supported the hypothesis that combined microbial-Fe(0) systems yield a better end-product distribution. This beneficial effect was not observed to change with varying hydraulic retention times.

4. The column experiments showed that there is potential for indigenous soil microbes to colonize Fe(0) and enhance treatment performance. Even though the sand in the autoclaved continuous-flow column had been autoclaved three times, indigenous soil microbes were able to selectively colonize the Fe(0) filings. Thus, the main advantage of bioaugmentation may be to shorten the acclimation period required for microbial colonization of Fe(0).

Conclusions from the rotating disk electrode and the effect of temperature experiments (Jennifer Ginner's thesis, Appendix B) include:

5. The reduction of nitrate at an oxide-free RDE is limited by the chemical reaction at the bare iron surface. However, this may not be true in batch experiments or field scale sites where the iron surface is covered with iron oxides and impurities. Iron oxides present a physical barrier that may increase the size of the diffusion layer between the bulk solution at the pure iron metal surface. This larger diffusion layer may cause the reduction of nitrate to be controlled by mass transport to the iron surface rather than the chemical reaction at the iron surface.

6. Reduction of nitrite at an oxide-free RDE is influenced by mass transport to the bare iron surface. Mass transport may have a larger influence in the field because the iron surface is covered with iron oxides and impurities.

7. Temperature affected the removal rate of both nitrate and nitrite by iron metal in batch systems. However, the removal rate of nitrite was much faster than the removal rate of nitrate at all temperatures tested. The activation energy for nitrate removal by iron metal in batch systems was 36.3 ± 9.08 kJ mol^{-1}, slightly indicative of surface-reaction control. The activation energy of nitrite removal by iron metal in batch system was 23.8 ± 3.95 kJ mol^{-1}, slightly indicative of mass transport control or mixed control. The batch temperature study indicated that nitrate removal by iron metal requires greater activation energy than nitrite removal.

LIST OF REFERENCES

Daniels, L., N. Belay, B. Rajagopal, and P. Weimer (1987). "Bacterial Methanogenesis and Growth from CO_2 with Elemental Iron as the Sole Source of Electrons." *Science.* 23: 509-511.

Grittini, C., M. Malcomson, Q. Fernando, and N. Korte (1995). "Rapid Dechlorination of Polychlorinated Biphenyls on the Surface of a Pd/Fe Bimetallic System." *Environmental Science and Technology*, 29: 2898-2900.

Huang, Chin-Pao, Hung-Wen Wang, and Pei-Chun Chiu (1998). "Nitrate Reduction by Metallic Iron." *Water Research*. 32: 2257-2264.

Kapoor, A. and T. Viraraghavan. (1997). "Nitrate Removal from Drinking Water-Review." *Journal of Environmental Engineering*. 123(4): 371-380.

Mirvish S. (1985). "Gastric cancer and salivary nitrate and nitrite", *Nature, 315* : 461-462.

Nolan, B. T., B. C. Ruddy,. K. J. Hitt, and D.R. Helsel. (1997). "Risk of nitrate in groundwaters of the United States - a national perspective". *Environmental Science and Technology.* 31: 2229-2236.

Powell, R. M and R. W. Puls (1997). "Proton Dissolution of Intrinsic or Augmented Aluminosilicate Minerals for in Situ Contaminant Remediation by Zero-Valence-State Iron." *Environmental Science and Technology.* 31: 2244-2251.

Scherer, M.M., B. A. Balko, and P. G. Tratnyek. (1998). "The Role of Oxides in Reduction Reactions at the Metal-Water Interface", in: Mineral-Water Interfacial reactions: Kinetics and Mechanisms, D. Sparks and T. Grundl, Editors. 1998, ACS Symposium Series No. 715, American Chemical Society: Washington, DC. p. 301-322.

Schreier, C. G. and M. Reinhard (1995). "Catalytic Hydrodehalogenation of Chlorinated Ethylenes Using Palladium and Hydrogen for the Treatment of Contaminated Water." *Chemosphere*, 31(6): 3475-3487.

Till, B. A., L. J. Weathers, and P.J. Alvarez. (1998). "Fe(0)-Supported Autotrophic Denitrification." *Environmental Science and Technology.* 32: 654-659.

Weathers, L. J., G. F. Parkin, and P. J. J. Alvarez. (1997). "Utilization of Cathodic Hydrogen as Electron Donor for Chloroform Cometabolism by a Mixed Methanogenic Culture." *Environmental Science and Technology*. 31(3): 880-885.

Yoshinari, T. and R. Knowles. (1976). "Acetylene Inhibition of Nitrous Oxide Reduction by Denitrifying Bacteria." *Biochemical and Biophysical Research Communications.* 69: 705-710.

Basic Information

Title:	Enhancing the abiotic degradation of trichloroethylene with bimetals
Project Number:	G-02
Start Date:	9/1/1998
End Date:	8/31/2000
Research Category:	Not Applicable
Focus Category:	Water Quality, None, None
Descriptors:	Water quality, degradation, bimetals
Lead Institute:	Iowa State Water Resources Research Institute
Principal Investigators:	Say Kee Ong

Publication

1. Yuan, W., T. Fryzek, W. Braida, and S.K. Ong. 2000. Reductive degradation of TCE using bimetallic reductants, (submitted to the Journal of Hazardous Materials)
2. Wan Chun Yuan, 2000, Degradation of trichloroethylene using iron, bimetals and trimetals, M.S. Thesis, Dept. of Civil and Construction Engineering, Iowa State University, Ames, IA, p 102.
3. Yuan, W., T. Fryzek, W. Braida, and S.K. Ong. 2000. Reductive degradation of TCE using bimetallic reductants, 2nd International Conference on Remediation of Chlorinated and Recalcitrant Compounds, May 22 - 25, Monterey, CA.
4. Suroso, I. and S. K. Ong. 2000. Treatment of nitrate-contaminated water with zero-valent iron and bimetals, 2nd International Conference on Remediation of Chlorinated and Recalcitrant Compounds, May 22 - 25, Monterey, CA.

Introduction

Remediation of groundwater contaminated with chlorinated organic compounds is needed as these compounds are generally toxic and are resistant to natural attenuation in the environment. Over the past decade, development of remediation technologies to remediate these contaminated sites has been a significant environmental priority. A commonly used method for remediating contaminated groundwater is the pump and treat technology, where water is pumped from the ground and treated *ex-situ*. The *ex-situ* treatment may involve air stripping and granular activated carbon adsorption. These technologies do not destroy chlorinated organic compounds but transfer them from one medium to another without solving the problem of final disposal. Some chlorinated organic compounds can be destroyed by advanced methods such as chemical oxidation using ozone with ultraviolet light and hydrogen peroxide. These alternatives are expensive and may not be applied as *in-situ* treatment. Some companies have tried *in situ* ozonation and found to have worked.

For *in-situ* treatment, reductive dechlorination using zero-valent metals is one of many emerging technologies that is currently being researched. Various metals such as Iron (Fe), Aluminum (Al), Tin (Sn), Magnesium (Mg) and Zinc (Zn) have been used to degrade chlorinated organic compounds (Boronina and Klabunde, 1995; Warren et al., 1995; Su and Puls, 1999). Zero-valent iron is the most common metal used. In a study by Gillham and O'Hannesin (1994), zero-valent iron was used to degrade 14 halogenated aliphatics including TCE. They found that the degradation rate constants appeared to be directly proportional to the surface area of the iron. In another study, Orth and Gillham (1996) found that the first-order rate constants of TCE degradation were relatively insensitive to the initial concentrations of TCE of 1.3 to 61 mg/L. Since dehalogenation apparently occurs at the Fe/H_2O interface, transport of the compound to the iron surface must be involved before the compound can be reduced (Matheson and Tratnyek, 1994). The half-lives of TCE using zero-valent iron are in the order of several days. Because the degradation rate using iron alone is slow, research emphasis has been focused on the use of a modified iron, such as the palladium-plated iron granules (Boronina and Klabunde, 1995; Liang et al., 1997; and Muftikian et al., 1995) and copper-plated iron or nickel-plated iron (Fryzek, 1997). Although much research has been done, the mechanisms and kinetics of reductive degradation using zero-valent metals are still unclear. There are only a few studies investigating the effects of plated metal concentration on iron and the effects of water quality on the degradation of TCE. In addition, the reactive life of the zero-valent iron or plated iron over long-term application is still unknown. Regardless of the possible negative effects of groundwater quality on the zero-valent iron or bimetals, this technology has been applied at various contaminated sites throughout the US.

Objectives of This Study

The objectives of this study are:

1) To determine the optimal concentrations of copper, nickel, and nickel/copper plated on the zero-valent iron to maximize the degradation of TCE,

2) To assess the effects of various anions in groundwater that may have an impact on TCE degradation with iron, bimetals and trimetals.

METHODS AND MATERIALS

Chemicals

Chemicals used were TCE (99.9%, Fisher Scientific, Pittsburgh, PA), and electrolytic iron powder (Fisher Scientific, Pittsburgh, PA). Calibration standards were prepared for TCE and for intermediate degradation compounds. Standards for the intermediate degradation compounds were cis-1,2-DCE (1000 μg/ml in methanol), trans-1,2- DCE (200 μg/ml in methanol), 1,1- DCE (200 μg/ml in methanol), and VC (200 μg/ml in methanol). All the intermediate compounds were purchased from Supelco (Bellefonte, PA). A mixed gas standard containing 100 ppm by moles of ethylene, 1-butene, 1-hexene, 1-pentene and propylene were purchased from Scotty (Deerfield, IL).

Preparation of bimetallic and trimetallic reductants

Iron used in the experiments was pretreated by soaking with 100 ml of 5% (v/v) H_2SO_4 for 60 minutes. The acid-washed iron was filtered with a 1 micron glass fiber filter and rinsed 3 times with 50 ml of nanopure water, 2 times with 96% ethanol, and one time with 99.6% acetone. The iron was then dried in an oven at $32\pm2°$ C for 12 hours. The dried acid-washed iron was kept under N_2 atmosphere in aluminum crimped cap bottle with Teflon-lined rubber septa.

To prepare bimetals and trimetals, a cold electrodeless method was used. About 50 to 100 gm of iron was acid-washed and rinsed with nanopure water as described above. The acid–washed iron was then soaked in 100 ml of copper sulfate or nickel sulfate or a mixture of copper and nickel sulfate solution depending on the bimetals and trimetals that were to be prepared. Different masses of copper and nickel were plated onto the iron by using different solution concentrations, the contact times between the iron and the solution and with or without agitation (see Table 3.1). The plated-iron was then filtered with a 1 micron glass fiber filter and rinsed 5 times with 50 ml nanopure water. Five or ten *grams* of bimetal or trimetal were immediately placed in a 60 ml glass serum vials with 25 ml nanopure water and 0.175 ml of 1,100 mg/L saturated TCE solution. The vials were immediately closed with an aluminum crimp cap with Teflon-lined rubber septa. The contents of copper and nickel on the iron were determined by acid digesting the plated-iron and the acid-digested solution analyzed using atomic absorption spectrophotometer (Smith-Hieftj 12 Model 857, Instrumentation Laboratory Inc., Lexington, MA or a GBC 932_{plus} atomic absorption spectrometer, Victoria, Australia).

Batch experiments

Each experimental run consisted of 6 or 7 60 ml glass serum vials with an equivalent number of control vials. Experiments were also conducted using a single 160 ml glass serum vial along with a control vial. With 160 ml glass serum vial, 20 gm of metals were added to 100 ml nanopure water and 0.7 ml of 1,100 mg/L saturated TCE. Each vial was prepared

according to the procedure described above. TCE concentrations in the vials ranged from 5-8 mg/L. All vials were rotated at 12 rpm using a tumbler. The experiments were conducted at a temperature of 21 ± 0.5°C. The control vials contained only TCE-contaminated solution without the reductants.

Table 3.1 Summary of Copper and Nickel Contents for Various Plating Conditions

Sample Identification	Iron Used (gm)**	Copper Sulfate Added (gm)	Nickel Sulfate Added (gm)	Reaction Time Before Rinse (minutes)	Copper Content in Iron (ppm)	Nickel Content in Iron (ppm)
Fe	50				643	396
FeCu1	50	1.271		5	9,970	396
FeCu3	50	5.004		5	29,791	396
FeCu5	50	9.939		5	48,520	396
FeCu7	75	34.689		5	108,341	396
FeCu8	75	18.832		5	64,836	396
FeCu6	50	15.073		5	80,585	396
FeCu9	75	27.637		5	92,559	396
FeCu11	75	38.559		5	138,063	396
FeNi2	100		14.971	120	643	1,083
FeNi3	60		13.304	30*	643	1,745
FeNi4	60		18.85	30*	643	2,486
FeNi5	75		28.641	45*	643	5,391
FeNi6	50		37.375	20*	643	6,417
FeNi1	100		18.83	600	643	9,360
FeNi7	50		57.327	20*	643	17,613
FeCuNi1	50	15.039	32.758	10*	83,643	21,375
FeCuNi2	50	15.073	19.872	10*	82,192	20,548
FeCuNi3	50	14.989	12.206	30*	73,235	11,000
FeCuNi4	50	12.073	9.619	30*	55,044	7,786
FeCuNi5	50	9.413	6.198	30*	41,740	3,953
FeCuNi6	50	3.18	5.999	10*	17,306	3,638

* in an Innova 2000 platform shaker (New Brunswick Scientific, Edison, NJ) at 250 rpm

** in 100 mL of nanopure water

At selected intervals, one control bottle and a reaction vial were removed from the tumbler. Headspace concentrations were measured by directly injecting 0.5 ml of headspace sample into a Hewlett-Packard 5890 II gas chromatograph (GC) (Acondale, PA) with a flame ionization detector. Aqueous concentrations were determined by transferring 0.2 ml of aqueous samples to a 1.8 ml vial which was sealed with an aluminum crimp cap. After reaching equilibrium, 0.5 ml of the headspace was analyzed by the GC. Based on Henry's Law constant, the concentration in aqueous phase was estimated from the headspace concentration. The GC had a Simplicify-5, 0.32 mm x 30 mm, capillary column (Supelco Inc., Bellefonte, PA) and. The oven program was kept at a temperature of 30°C for 3 minutes. Injection port and detector temperature was 150°C and 250°C, respectively.

pH measurements before and after each experiment were conducted using an Accumet 25 pH meter (Fisher Scientific, Pittsburgh, PA). To measure the aqueous copper or nickel concentration at the end of the experiments, the solution was first filtered through a 1 micron glass fiber filter. The copper or nickel concentration was measured by atomic absorption spectrophotometer after the filtered solution was acid digested with nitric acid.

To study the effects of anions, solutions were prepared with 50, 400, 800 mg/L HCO_3^-; 0.1, 1, 5 mg/L PO_4^{3-}; 20, 100, 400 mg/L SO_4^{2-}; and 5, 20, 60, 200 mg/L NO_3^-. TCE concentrations ranged from 5-8 mg/L. All vials were mixed thoroughly using a twist shaker. Temperature was measured by a thermometer and was 23.5 ± 0.5°C for all the experiments. The control vials contained only TCE-contaminated solution without the reductants.

At selected intervals, the control vials and reaction vials were removed from the shaker. Headspace concentrations were measured by directly injecting 0.5 mL of headspace sample into a Hewlett-Packard 5890 II gas chromatography (GC) (Acondale, PA) with a flame ionization detector. Liquid concentrations were analyzed by transferring 0.2 mL of aqueous samples to a 1.8 mL vial which was sealed with an aluminum crimp cap. After reaching equilibrium, 0.5 ml of the headspace was analyzed by the GC. Using the Henry's Law constant for the compound, the concentration in the aqueous phase was estimated from the headspace concentration. The column for the GC was a Simplicify-5 0.32mm×30mm capillary column (Supelco Inc., Bellefonte, PA). The oven program was kept at a temperature of 30°C for 3 minutes. Injection port and detector temperatures were 150°C and 250°C, respectively. Carrier gas used was helium and it was kept at a constant rate of 3.97 mL/min.

pH measurements before and after each experiment were conducted using an Accumet 25 pH meter (Fisher Scientific, Pittsburgh, PA). The anion concentrations before and after the experiments were measured by a DIONEX ion chromatograph (Sunnyvale, CA). To measure copper and nickel concentrations in the aqueous phase at the end of the experiments, the solution was first filtered through a 1 micron glass fiber filter. The copper and nickel concentrations were measured by atomic absorption after the clean solution was acid digested with nitric acid.

RESULTS AND DISCUSSIONS

Effects of Bimetals Content

For the bimetal Fe/Cu, the amount of copper plated onto the iron ranged from 1.0% (weight precentages) to 13.8% with the cold electrodeless approach. For the bimetal Fe/Ni, the amount of nickel plated ranged from 0.1% Ni to 1.8% Ni. For the trimetal Fe/Cu/Ni, the percent of copper plated ranged from 1.7% to 8.3% while the percent of nickel ranged from 0.3% to 2.1%. Figure 4.1 presents typical results for the degradation of TCE by Fe, Fe/Cu (with 9.26% Cu), Fe/Ni (with 0.25% Ni) and Fe/Cu/Ni (with 4.17% Cu and 0.4% Ni). Included in Figure 4.1 are the byproducts of TCE. As observed in Figure 4.1, the half-life of TCE with iron was approximately 10 hours while the half lives of TCE for Fe/Cu and Fe/Ni were approximately 5 hours and 1 hour, respectively. The half-life for the reaction of TCE with Fe/Cu/Ni was found to be approximately 0.5 hour. The reactions were assumed to be pseudo first order and the first order reaction rate constants were estimated. Table 4.1 summarized the first order degradation rate constants and their 90% confidence intervals for the various bimetal and trimetal experiments.

Reaction of TCE with Fe/Cu

The first order degradation rate constants of TCE with different copper contents on zero-valent iron are shown in Figure 4.2. The first order degradation rate constants increased with increasing copper concentration and reached a maximum degradation rate of 0.64±0.09 hr^{-1} at approximately 9.26% copper. Above a copper content of 9.26%, the degradation rates decreased rapidly. Overall, the degradation rate constants for Fe/Cu were 2-9 times larger than that of zero-valent iron.

In the experiments with iron, cis-1, 2-DCE (6.07% of the total initial carbon mass), trans-1, 2-DCE (0.66%) and 1-1-DCE (1.90%) were detected as intermediate daughter products. The dominant end product generated was ethylene. A small amount C_4H_8 (2.8%) was also detected. Trace amounts of C_3-C_6 hydrocarbons were detected when the headspace sample was analyzed by GC/MS. A GC/MS chromatograph is shown in Figure 4.3. In the experiments with Fe/Cu, cis-1,2-DCE, trans-1,2-DCE and 1,1-DCE were not detected. The end products for the Fe/Cu treatment were ethylene (28.5 - 60.6%) and C_3H_6 (0.42 - 1.9%) and trace amount of C_3-C_6 hydrocarbons. The production of ethylene and C_4H_8 were found to be less than that of Fe alone. For most of the reactions with Fe/Cu, the final pH values were found to be slightly lower than the initial pH values (Table 4.1).

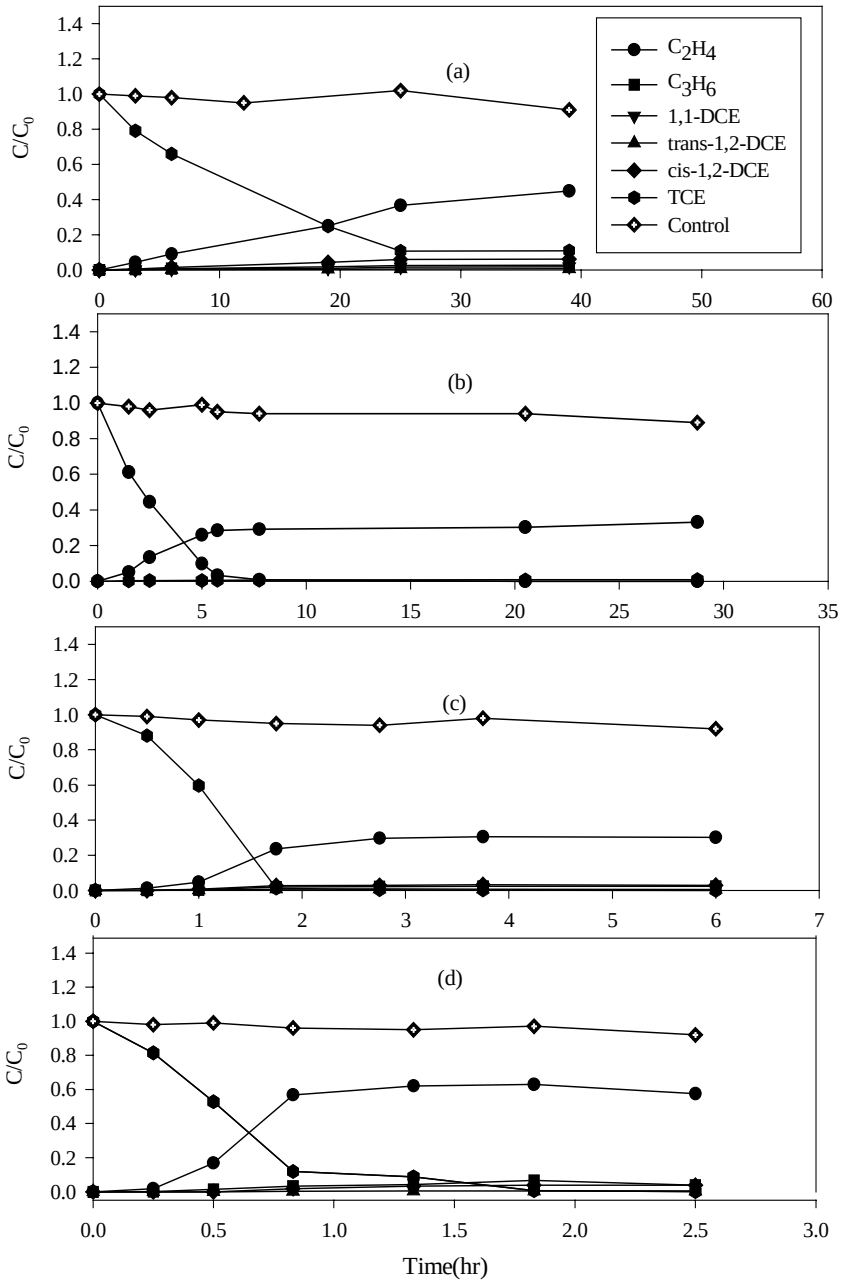

Figure 4.1. Degradation of TCE with (a) Zero-valent Iron; (b) Fe/Cu (with 9.26% Cu); (c) Fe/Ni (with 0.25%Ni); (d) Fe/Cu/Ni (with 4.17% Cu and 0.4% Ni)

Table 4.1 TCE Degradation Rate Constants with Fe, Fe/Cu, Fe/Ni and Fe/Cu/Ni

Sample Identification	Mass of Metal Used (gm)	Initial pH	Final pH	Control pH	Degradation Rate ± 90% CI (hr-1)	R^2
Fe	10.002*	8.76	9.62	8.85	0.064±0.012	0.91
FeCu1 (1.00% Cu)	10.000*	6.27	9.12	6.33	0.15±0.03	0.97
FeCu3 (2.98% Cu)	10.006*	6.27	9.32	6.33	0.16±0.02	0.99
FeCu5 (4.85% Cu)	5.051	5.97	6.51	6.11	0.28±0.04	0.97
FeCu6 (8.06% Cu)	5.009	5.91	5.58	5.81	0.33±0.06	0.88
FeCu7 (10.83% Cu)	5.053	5.91	5.44	5.81	0.45±0.12	0.86
FeCu8 (6.48% Cu)	5.033	5.80	6.02	5.94	0.29±0.04	0.96
FeCu9 (9.26% Cu)	5.017	5.80	5.71	5.94	0.64±0.09	0.96
FeCu11 (13.81% Cu)	5.002	5.73	5.50	5.68	0.16±0.01	0.97
FeNi1 (0.94% Ni)	5.000	7.01	5.10	7.26	1.36±0.24	0.97
FeNi2 (0.11% Ni)	5.001	7.01	6.23	7.26	0.66±0.12	0.92
FeNi3 (0.17% Ni)	5.012	5.62	6.04	5.51	1.41±0.27	0.96
FeNi4 (0.25% Ni)	5.023	5.62	5.72	5.51	1.90±0.29	0.90
FeNi5 (0.54% Ni)	5.021	5.62	5.14	5.61	0.37±0.26	0.94
FeNi7 (1.76% Ni)	5.025	5.78	5.56	5.80	0.98±0.18	0.94
FeCuNi1 (8.26% Cu, 2.14% Ni)	20.044**	5.88	5.42	5.70	1.56±0.45	0.90
FeCuNi2 (8.22% Cu, 2.05% Ni)	20.132**	5.88	5.28	5.70	1.97±0.39	0.97
FeCuNi3 (7.32% Cu, 1.10% Ni)	20.068**	6.3	6.20	6.39	2.37±0.42	0.97
FeCuNi4 (5.50% Cu, 0.78% Ni)	20.096**	6.3	6.02	6.39	2.85±0.43	0.99
FeCuNi5 (4.17% Cu, 0.40% Ni)	20.072**	6.3	6.36	6.39	3.20±0.51	0.98
FeCuNi6 (1.73% Cu, 0.36% Ni)	20.068**	5.36	5.11	5.20	1.28±0.34	0.93
Fe***					0.044±0.005	0.98
FeCu I(0.92% Cu)***					0.155±0.037	0.94
FeCu II (4.25% Cu)***					0.204±0.02	0.98

	9	
FeNi I (0.14% Ni)***	0.382±0.10	0.94
	0	
FeNi II (0.33% Ni)***	0.734±0.25	0.94
	1	
FeCuNi I (1.13% Cu, 0.16%	0.119±0.02	0.94
Ni)***	6	

* in 50 mL
** in 100 mL, others in 25 mL (ratios of metal mass/solution volume are the same)
*** unpublished data (Braida, 1999)

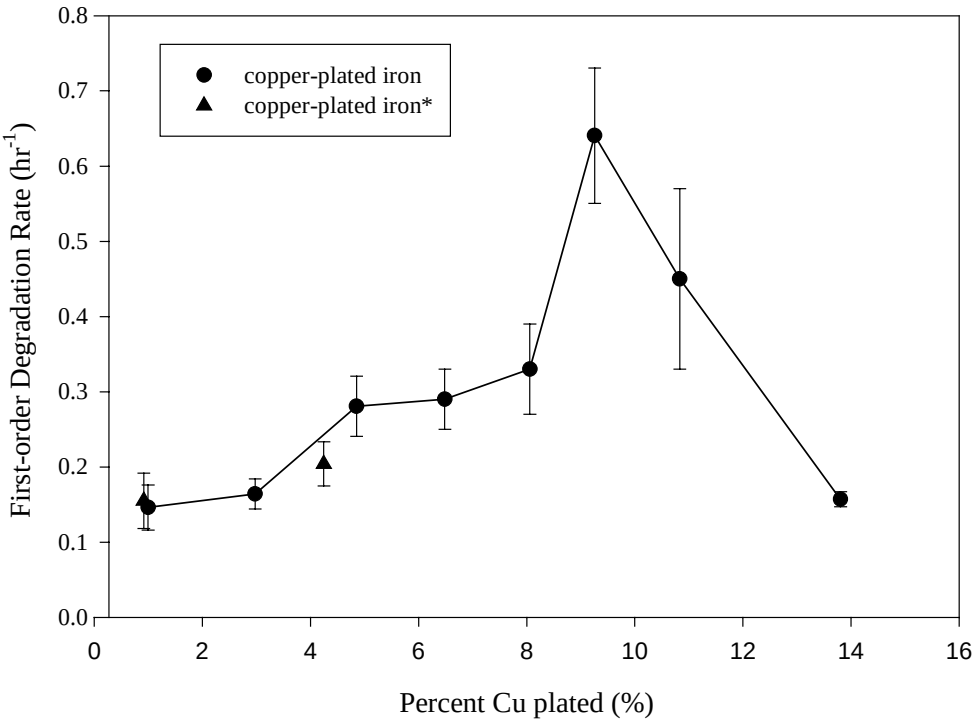

Fig 4.2 First Order Degradation Rate Constants (with 90% C.I.) as a Function of Percent Cu on Iron (* unpublished data from Washington's data)

Reaction of TCE with Fe/Ni

The degradation of TCE with various nickel contents on zero-valent iron is plotted as shown in Figure 4.4. The degradation rate constants with Fe/Ni were found to be larger than that of Fe/Cu and 30 times larger than that of zero-valent iron. The maximum degradation rate constant was found to be 1.90 ± 0.29 hr^{-1} for a Ni concentration of 0.25%. With Ni concentration greater than 0.25%, the degradation rates were found to decrease (see Figure 4.4).

Except for 1,1-DCE, the intermediate daughter products detected were cis-1,2-DCE (2.09-3.34%) and trans-1,2-DCE (0.58-2.48%). The final end products were the same as Fe/Cu with ethylene and trace amounts of C_3-C_6 hydrocarbons. However, the production of ethylene was found to be slightly less than that of Fe/Cu but the production of C_4H_8 (0.26-2.4%) was more than that of Fe/Cu. The final pH values were found to be slightly higher than the initial pHs.

Reaction of TCE with Fe/Cu/Ni

The degradation of TCE was found to be significantly enhanced with the trimetal Fe/Cu/Ni as compared to Fe/Ni and Fe/Cu (see Table 4.1 and Figure 4.4). The first order degradation rate constants were found to be 20-50 times larger than those of zero-valent iron. Based on the limited number of experiments for Fe/Cu/Ni system, the maximum degradation rate constant was obtained for a copper concentration of 4.17% and a nickel concentration of 0.40%. The copper concentration of 4.17% was lower than the copper content of 9.26% for the maximum degradation by Fe/Cu, but the nickel concentration of 0.40% was higher than the nickel content of 0.25% for the maximum degradation by Fe/Ni. Increasing the copper and nickel content beyond these concentrations resulted in lower degradation rate constants for TCE (see Figure 4.4).

The intermediate products produced using Fe/Cu/Ni were similar to that of Fe/Ni. Only cis-1,2-DCE (2.6-7.5%) and trans-1,2-DCE (0.36-0.56%) were found during the experiments. The ethylene production (40-58%) was found to be more than that of Fe/Ni. The final pH values were found to be higher than the initial pH values.

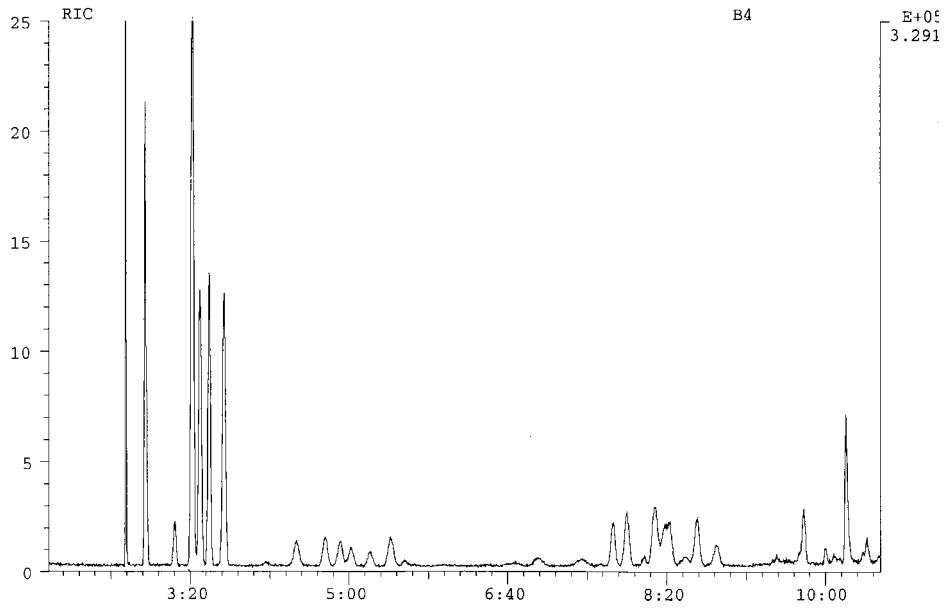

Figure 4.3 Typical GC/MS Chromatograph for the Degradation of TCE with Zero-valent Iron (Key: 1 – ethane (C_2H_6); 2 – ethylene (C_2H_4); 3 - C_3H_6; 4, 6 and 7 - C_4H_8; 5 - C_4H_{10}; 8, 9, 10, 11, and 13 - C_5H_{10}; 12 - C_5H_{12}; 14 - C_6H_{14}; 15, 16, 17, 18, and 19 - C_6H_{12}; 20 and 21 - C_6H_{10})

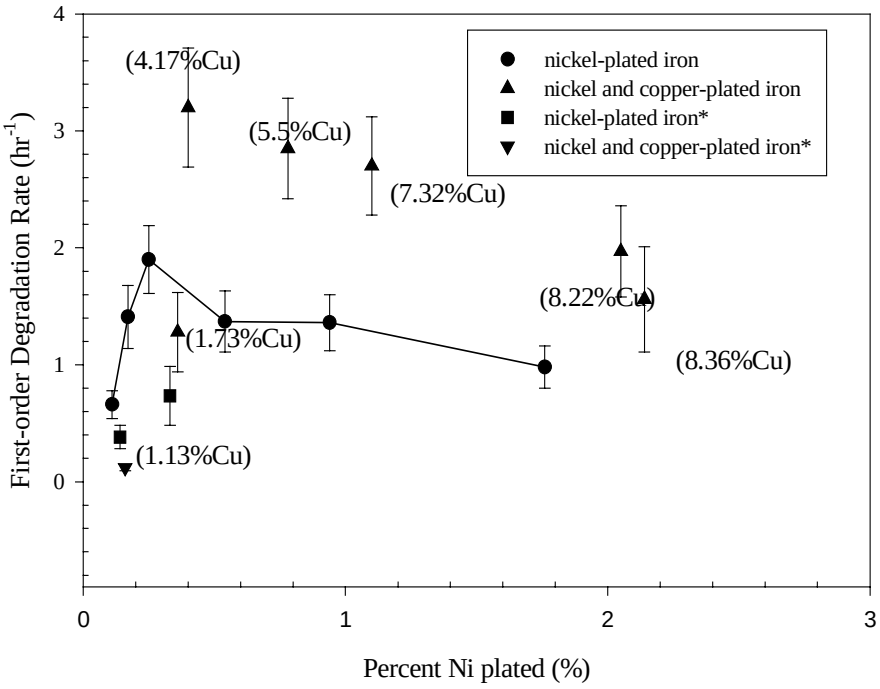

Figure 4.4. First-order Degradation Rate Constants of TCE as a Function of Percent Cu on Iron (* unpublished data from Washington Braida, 1999)

Discussion on Effects of Bimetal Contents

Degradation of TCE with Fe/Ni and Fe/Cu was faster than zero-valent iron while the reaction with Fe/Cu/Ni was significantly faster than Fe/Ni and Fe/Cu (Table 4.1). The enhanced reactivity of Fe/Ni was similar to the results of other researchers (Fryzek, 1998; Fennelly and Robert, 1998; Appleton, 1996). Ethylene production observed in decreasing amounts with different reductants were as follows: zero-valent iron, Fe/Cu/Ni Fe/Ni, and Fe/Cu. The production of C_4H_8 *was* similar for all reductants while the production of partially dechlorinated products (sum of trans-1,2-DCE, cis-1,2-DCE and 1,1-DCE) in decreasing order were zero-valent iron followed by Fe/Ni, Fe/Cu/Ni and Fe/Cu. In the case of Fe/Cu, no cis-1,2-DCE, trans-1,2-DCE and VC were detected while these compounds were detected for zero-valent iron, Fe/Ni and Fe/Cu/Ni. Because a very small mass of partially dehalogenated products was produced, one may speculate that TCE on the iron surface was first reduced to the partially dehalogenated products, then these intermediate products continue to be reduced to ethylene. Sometimes the partially dechlorinated products were set free from the iron surface before they were degraded to ethylene. The lack of production of partially dechlorinated compounds during the degradation with Fe/Cu indicated that the surface of Fe/Cu somehow was able to retain the partially dechlorinated compounds longer until they were fully degraded to ethylene. Therefore, sorption of TCE on the surface of Fe/Cu may also contribute toward the faster disappearance of TCE and the lower ethylene production as compared to the zero-valent iron.

As for the formation of C_4 alkenes and alkanes, one possible reason for the formation C_4 alkanes and alkenes is the potential coupling of chloroethyl radicals which results in the formation of C_4 compounds as suggested by Fennelly and Roberts (1998). This proposed pathway can not explain the formation of hydrocarbon compounds with an odd carbon number such as C_3 or C_5 compounds. In order to form C_3 or C_5 compounds through the degradation of TCE, the double bond of C=C has to be broken to form single carbon radicals. Hardy and Gilham (1996) examined the formation of hydrocarbons from aqueous solutions (no chloroethenes present) in the presence of metallic iron. They reported the formation of methane, ethane, ethene, propane, propene, butene isomers, and C_5 compounds and proposed that CO_2 be reduced to from these hydrocarbons through Fisher-Tropsch synthesis. Campbell et al. (1997) confirmed that the carbon in the observed C_1 to C_5 compounds was derived predominantly form the TCE using $^{14}C_2$-labelled TCE and GC-MS analysis. However, the studies by Deng et al. (1997) indicated that aqueous CO_2 was not a major source of carbon for the C_1 to C_5 compounds and carbide carbon in the iron appeared to be the most likely carbon source for the production of the background hydrocarbons. In this study, control experiments without TCE added showed that no C_1 to C_5 compounds was detected in water/iron batch system. Therefore, the carbon in the C_1 to C_5 compounds was derived predominantly from the TCE.

The degradation of TCE by iron may be explained by the reduction of TCE with zero-valent iron serving as the source of electrons from the corrosion of iron. The increased degradation rate of Fe/Cu in comparison to zero-valent iron may be explained by the galvanic cell concept (Fryzek, 1998). The standard electrode potential for Fe/Cu

cell is 0.78 V which is higher than that of iron with a standard hydrogen electrode (0.44V). This means that the corrosion of iron for the Fe/Cu bimetal may be faster than that of iron alone. This may be one of the reasons for the observed increased degradation rate for Fe/Cu. However, in the case of Fe/Ni, the reaction rate of Fe/Ni was much faster than that of Fe/Cu even though the standard electrode potential for Fe/Ni cell (0.21V) is much lower than that of Fe/Cu. This discrepancy would suggest that the galvanic cell approach may not be true and that other factors might contribute toward the enhanced degradation rate. Another possible explanation is that nickel may act as a hydrogenolysis catalyst. Nickel is known to absorb hydrogen gas and other poisons and this in turn may remove the hydrogen gas from the surface of iron and increase the rate of iron corrosion. If this is true, then increasing the Ni content will increase the removal of hydrogen from the surface. However, increasing the Ni content on the surface of iron may result in a lower exposed surface area of iron and therefore will result in a decrease in the reaction rates. Cheng et al. (1997) proposed that hydrogen gas intercalated in a palladium lattice was the powerful reducing agent that dechlorinated organic compounds that were absorbed on the surface of palladized electrodes. For the trimetal Fe/Cu/Ni, the combined effects of Fe/Cu and Fe/Ni may be the reason for the enhanced degradation rate. In summary, there may be several reasons for the enhanced effects of Cu and Ni on the degradation of TCE. These may include the galvanic effect, enhanced adsorption of TCE, and the removal of hydrogen from the surface of iron. As indicated above, the role of Cu and Ni on the degradation reaction of TCE is still unknown.

A concern with the use of bimetallic (Fe/Cu and Fe/Ni) and trimetallic (Fe/Cu/Ni) for the remediation of contaminated groundwater is the leaching of Cu and Ni to the groundwater. A set of experiments using bimetals were conducted for 5 days and the amount of Cu and Ni leached into the aqueous phase were 0.0043%-0.075% and 0.0093%-0.043% respectively of the initial mass of Cu and Ni present in the bimetals. The low release of Cu and Ni in the aqueous phase indicates that Cu and Ni may not be directly involved in the reductive reaction.

Effects of Anions

The copper and nickel contents of the bimetal Fe/Cu and Fe/Ni were 3.86% Cu and 0.14% Ni, respectively. For the trimetal Fe/Cu/Ni, the copper and nickel contents were 7.91% Cu and 1.72% Ni, respectively. The results on the effects of various anions on TCE degradation are summarized in the form of first-order degradation rates and are presented in Table 4.2 – 4.6. Table 4.2 presents the degradation rates for Fe/Cu/Ni system while Table 4.3 presents the degradation rates for Fe/Ni. Tables 4.4 and 4.5 present the degradation rates for Fe/Cu and Fe. All of the degradation rate constants were reported with a 90% confidence intervals. The concentrations of various anions during the experiment were presented in Table 4.6.

4.2.1 Effect of NO_3^- on TCE Degradation Rate

For the trimetal Fe/Cu/Ni, the effects of NO_3^- were presented in Figure 4.5. At a confidence interval of 90%, the degradation rate of TCE in 5 mg/L NO_3^- solution ($8.87 \pm 3.38\ hr^{-1}$) was higher than that of de-ionized water ($2.15 \pm 0.58\ hr^{-1}$). For a nitrate

Table 4.2 Effects of Various Anions on the Dehradation of TCE with FeCuNi*

Sample Indentification	Mass of Metal (gm)	Initial pH	End pH	Degradation rate Constant ± 90% CI (hr-1)	R^2
Deionized Water	10.009	6.01	5.68	2.15±0.58	0.92
HCO_3^- (50 mg/L)	10.007	7.88	8.45	3.38±1.37	0.87
HCO_3^- (400 mg/L)	10.009	8.53	9.50	4.17±1.8	0.86
HCO_3^- (800 mg/L)	10.006	8.56	10.03	4.25±1.04	0.95
PO_4^{3-} (0.1mg/L)	10.007	7.46	6.36	4.7±1.97	0.88
PO_4^{3-} (1 mg/L)	10.008	7.38	6.50	5.32±1.99	0.89
PO_4^{3-} (5 mg/L)	10.010	6.75	6.10	5.57±1.46	0.96
SO_4^{2-} (20 mg/L)	10.005	6.08	5.87	5.37±1.7	0.92
SO_4^{2-} (100 mg/L)	10.007	5.94	5.68	5.99±1.95	0.91
SO_4^{2-} (400 mg/L)	10.009	5.72	5.58	5.25±0.89	0.97
NO_3^- (5 mg/L)	10.007	6.57	6.81	8.87±3.38	0.93
NO_3^- (20 mg/L)	10.007	6.23	7.90	6.06±2.05	0.91
NO_3^- (60 mg/L)	10.009	6.02	8.85	2.00±0.66	0.91
NO_3^- (200 mg/L)	10.013	5.89	8.62	0.012±0.0179	0.16

Table 4.3 Effects of Various Anions on the Degradation of TCE with FeNi*

Sample Indentification	Mass of Metal (gm)	Initial pH	End pH	Degradation rate Constant ± 90% CI (hr-1)	R^2
Deionized Water	10.007	6.01	5.98	0.645±0.195	0.9
HCO_3^- (50 mg/L)	10.008	7.88	8.01	0.488±0.055	0.99
HCO_3^- (400 mg/L)	10.006	8.53	8.49	0.545±0.121	0.94
HCO_3^- (800 mg/L)	10.005	8.56	8.72	0.705±0.152	0.95
PO_4^{3-} (0.1mg/L)	10.009	7.46	7.54	0.44±0.142	0.89
PO_4^{3-} (1 mg/L)	10.006	7.38	7.43	0.784±0.141	0.96
PO_4^{3-} (5 mg/L)	10.004	6.75	6.81	0.811±0.128	0.97
SO_4^{2-} (20 mg/L)	10.010	6.08	5.98	0.608±0.123	0.95
SO_4^{2-} (100 mg/L)	10.008	5.94	6.03	0.62±0.097	0.97
SO_4^{2-} (400 mg/L)	10.007	5.72	5.89	0.674±0.145	0.95
NO_3^- (5 mg/L)	10.011	6.57	6.74	0.585±0.087	0.97
NO_3^- (20 mg/L)	10.009	6.23	6.36	0.629±0.095	0.97
NO_3^- (60 mg/L)	10.011	6.02	5.89	0.276±0.062	0.94
NO_3^- (200 mg/L)	10.019	5.89	6.05	0.014±0.0068	0.21

*Nickel content was 0.14% (w/w)

Table 4.4 Effects of Various Anions on the Degradation of TCE with FeCu*

Sample Indentification	Mass of Metal (gm)	Initial pH	End pH	Degradation rate Constant ± 90% CI (hr-1)	R^2
Deionized Water	10.008	6.01	6.12	0.17±0.052	0.97
HCO_3^- (50 mg/L)	10.007	7.88	8.01	0.224±0.024	0.99
HCO_3^- (400 mg/L)	10.005	8.53	8.57	0.239±0.022	0.99
HCO_3^- (800 mg/L)	10.005	8.56	8.49	0.262±0.015	1.0
PO_4^{3-} (0.1mg/L)	10.004	7.46	7.51	0.195±0.049	0.93
PO_4^{3-} (1 mg/L)	10.003	7.38	7.36	0.197±0.045	0.94
PO_4^{3-} (5 mg/L)	10.002	6.75	6.84	0.205±0.051	0.93
SO_4^{2-} (20 mg/L)	10.007	6.08	6.11	0.205±0.047	0.94
SO_4^{2-} (100 mg/L)	10.005	5.94	5.87	0.21±0.042	0.95
SO_4^{2-} (400 mg/L)	10.005	5.72	5.81	0.234±0.038	0.97
NO_3^- (5 mg/L)	10.007	6.57	6.68	0.235±0.057	0.93
NO_3^- (20 mg/L)	10.008	6.23	6.32	0.23±0.058	0.93
NO_3^- (60 mg/L)	10.010	6.02	5.97	0.166±0.068	0.83
NO_3^- (200 mg/L)	10.016	5.89	6.04	0.0064±0.0218	0.051

*Copper content was 3.86% (w/w)

Table 4.5 Effects of Various Anions on the Degradation of TCE with Fe

Sample Indentification	Mass of Metal (gm)	Initial pH	End pH	Degradation rate Constant ± 90% CI (hr-1)	R^2
Deionized Water	10.010	5.99	6.12	0.0484±0.0128	0.9
HCO_3^- (50 mg/L)	10.010	7.88	9.89	0.028±0.007	0.96
HCO_3^- (400 mg/L)	10.011	8.53	11.26	0.104±0.014	0.99
HCO_3^- (800 mg/L)	10.009	8.56	10.86	0.104±0.009	0.99
PO_4^{3-} (0.1mg/L)	10.008	7.46	9.4	0.0673±0.022	0.88
PO_4^{3-} (1 mg/L)	10.007	7.38	8.56	0.0689±0.019	0.91
PO_4^{3-} (5 mg/L)	10.009	6.75	8.02	0.11±0.039	0.87
SO_4^{2-} (20 mg/L)	10.006	6.08	9.11	0.034±0.006	0.96
SO_4^{2-} (100 mg/L)	10.008	5.94	9.86	0.060±0.015	0.93
SO_4^{2-} (400 mg/L)	10.009	5.72	9.56	0.072±0.016	0.94
NO_3^- (5 mg/L)	10.011	6.57	8.26	0.095±0.042	0.8
NO_3^- (20 mg/L)	10.011	6.23	9.36	0.030±0.011	0.86
NO_3^- (60 mg/L)	10.016	6.02	9.6	0.028±0.011	0.83
NO_3^- (200 mg/L)	10.023	5.89	6.34	0.027±0.002	0.99

Table 4.6 Concentration of NO_3^- During the Degradation of TCE

Type of Reductant	Time (hr)	NO_3^- Concen-tration (mg/L)	Time (hr)	NO_3^- Concen-tration (mg/L)	Time (hr)	NO_3^- Concen-tration (mg/L)	Time (hr)	NO_3^- Concen-tration (mg/L)
Fe	0	5	0	20	0	60	0	200
	2	4.89	2	17.95	2	33.34	2	27.46
	6.5	2.87	6.5	11.14	6.5	30.56	22	9.08
	16.5	2.5	16.5	7.56	16.5	27.73	32.5	8.28
	30.5	2.05	30.5	3.83	30.5	27.91	55	7.46
FeCu	0	5	0	20	0	60	0	200
	14	2.36	24	9.64	24	7.55	22	15.52
	24	0.77					32.5	9.74
							46.5	7.56
							55	5.55
FeNi	0	5	0	20	0	60	0	200
	1	3.94	3	9.95	1	24.44	22	5.82
	3	3.22	6	4.67	3	22.48	32.5	3.65
					6	21.8	46.5	3.16
					14	17.76	55	2.74
FeCuNi	0	5	0	20	0	60	0	200
	0.67	3.34	0.67	12.4	0.67	32.12	1.63	145.8
	0.83	2.42	0.83	3.27	0.83	5.76		
			1.33	2.98	1.33	1.4		

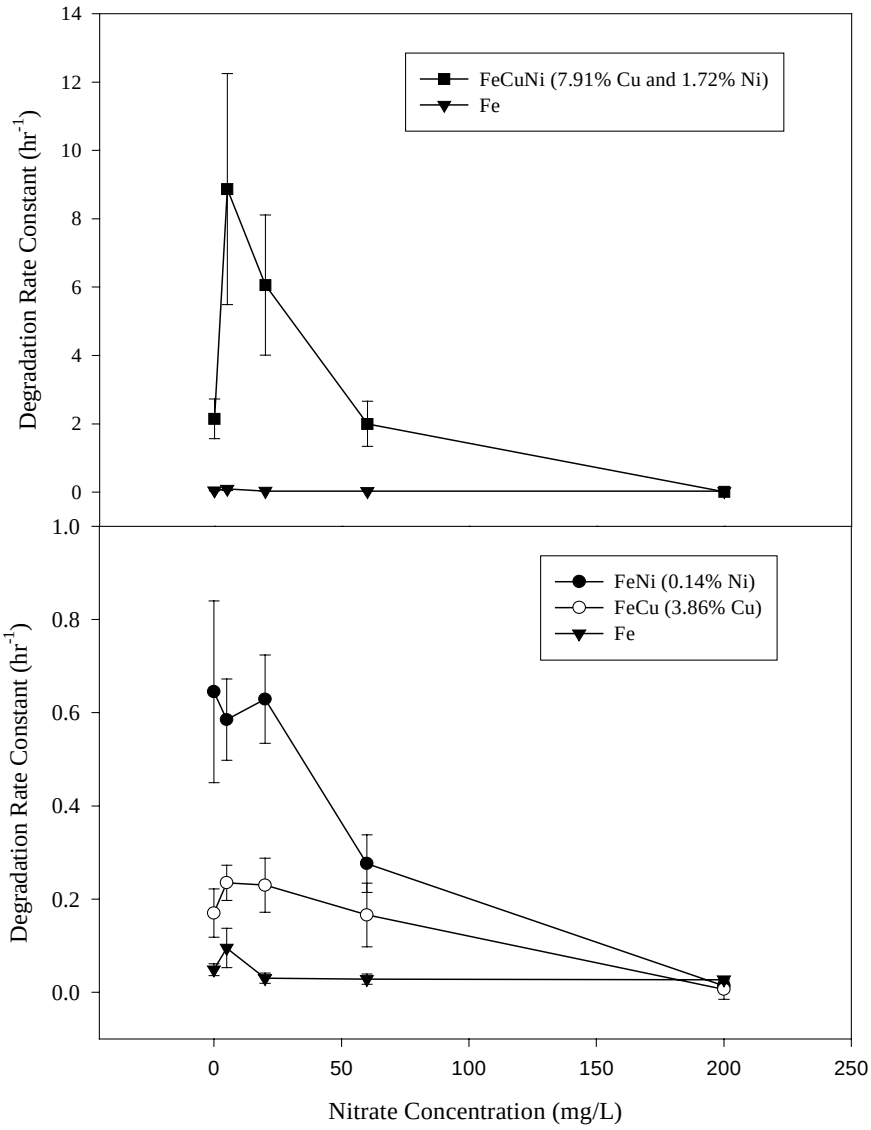

Figure 4.5. NO_3^- Effects on the TCE Degradation Rate Constant
(error bar - 90% confidence interval)

concentration of 20 mg/L, the TCE degradation rate decreased to 6.06±2.05 hr^{-1}. When the NO_3^- concentration increased to 60 and 200 mg/L, the TCE degradation rate constants were reduced to 2±0.66 hr^{-1} and 0.012±0.018 hr^{-1}, respectively. For a NO_3^- concentration of 200 mg/L, the TCE degradation rate was very slow and did not conform to a first-order reaction. After 1.6 hr of reaction time, the concentration of NO_3^- was found to be 146 mg/L. When concentrations of NO_3^- were 20 and 60 mg/L, at time 1.33 hr, 85% and 98% of NO_3^- was removed, respectively. Byproducts produced were found to be similar to that using de-ionized water only. Carbon mass balance was found to range from 55.4% to 68%.

For bimetal Fe/Ni, the first-order degradation rate constants were statistically similar at 90% confidence interval for a nitrate concentration of 20 mg/L and for de-ionized water. With a NO_3^- concentration of 60 mg/L, the TCE degradation rate decreased slightly to 0.276±0.062 hr^{-1}. When the NO_3^- concentration was 200 mg/L, the reaction rate was 0.014±0.0068 hr^{-1}. When the initial NO_3^- concentrations were 5mg/L, 20 mg/L, 60 mg/L and 200 mg/L, the final NO_3^- concentrations were 3.22 mg/L, 4.67 mg/L, 17.76 mg/L and 2.74 mg/L, respectively.

For bimetal Fe/Cu, the degradation rate constants were statistically similar at NO_3^- concentrations ranging from 0 mg/L to 60 mg/L. When the NO_3^- concentration was 200 mg/L, the degradation rate decreased to 0.0064±0.0218 hr^{-1}. NO_3^- concentration decreased from 5 mg/L, 20 mg/L, 60 mg/L and 200 mg/L to 0.77 mg/L, 9.64 mg/L, 7.55 mg/L and 5.55 mg/L, respectively.

For Fe only, TCE degradation rates were statistically similar at the 90% confidence level for NO_3^- concentrations ranging form 0 mg/L to 200 mg/L. At the end of the experiments, NO_3^- concentrations were 2.05 mg/L, 3.83 mg/L, 27.91 mg/L and 7.46 mg/L as compared to the initial NO_3^- concentrations of 5 mg/L, 20 mg/L, 60 mg/L and 200 mg/L, respectively.

In summary, competition between NO_3^- and TCE was present but did not affect the degradation rates of TCE using Fe/Ni and Fe/Cu until the concentration of NO_3^- was more than 60 mg/L for Fe/Cu and 20 mg/L for Fe/Ni. For Fe/Cu/Ni, nitrate enhanced the degradation rate of TCE but if concentration of NO_3^- was more than 60 mg/L, NO_3^- inhibited the degradation rate of TCE. Of the four reductants used (Fe/Cu/Ni, Fe/Ni, Fe/Cu and Fe). With 200 mg/L of NO_3^-, TCE degradation rates with Fe/Cu/Ni, Fe/Ni, Fe/Cu, and Fe were statistically similar. For NO_3^- concentration less than 200 mg/L, the degradation rates of TCE in order of highest to lowest were Fe/Cu/Ni > Fe/Ni > Fe/Cu > Fe.

Effects of HCO_3^- on TCE Degradation Rate

The exposure of trimetal Fe/Cu/Ni to water with HCO_3^- concentrations ranging from 50 mg/L to 800 mg/L (Figure 4.6) did not significantly affect the degradation rates of TCE at the 90% confidence interval as compared to that of de-ionized water. Similar results were also obtained for Fe/Ni and Fe/Cu. For Fe, 50 mg/L of HCO_3^- solution slightly inhibited the degradation rates of TCE at 90% confidence interval as compared to

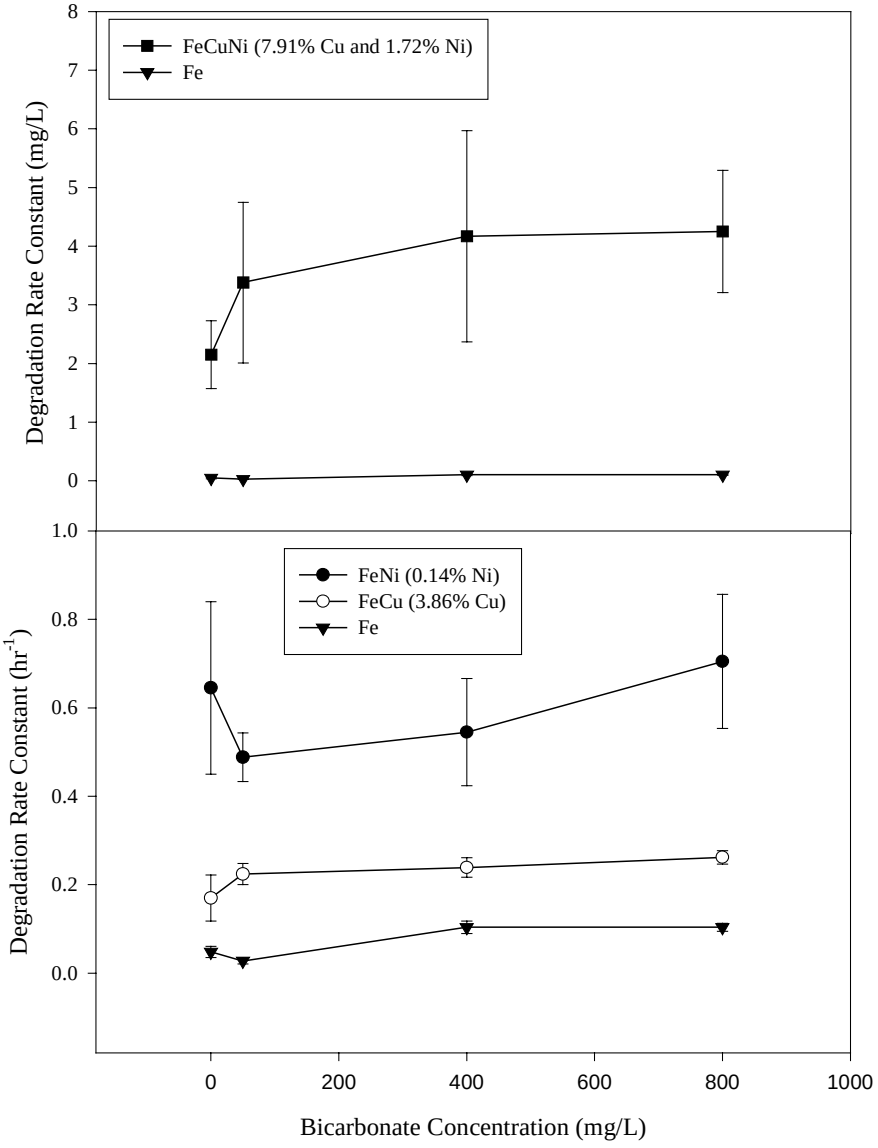

Figure 4.6. HCO_3^- Effects on the TCE Degradaion Rate Constant
(error bar - 90% confidence interval)

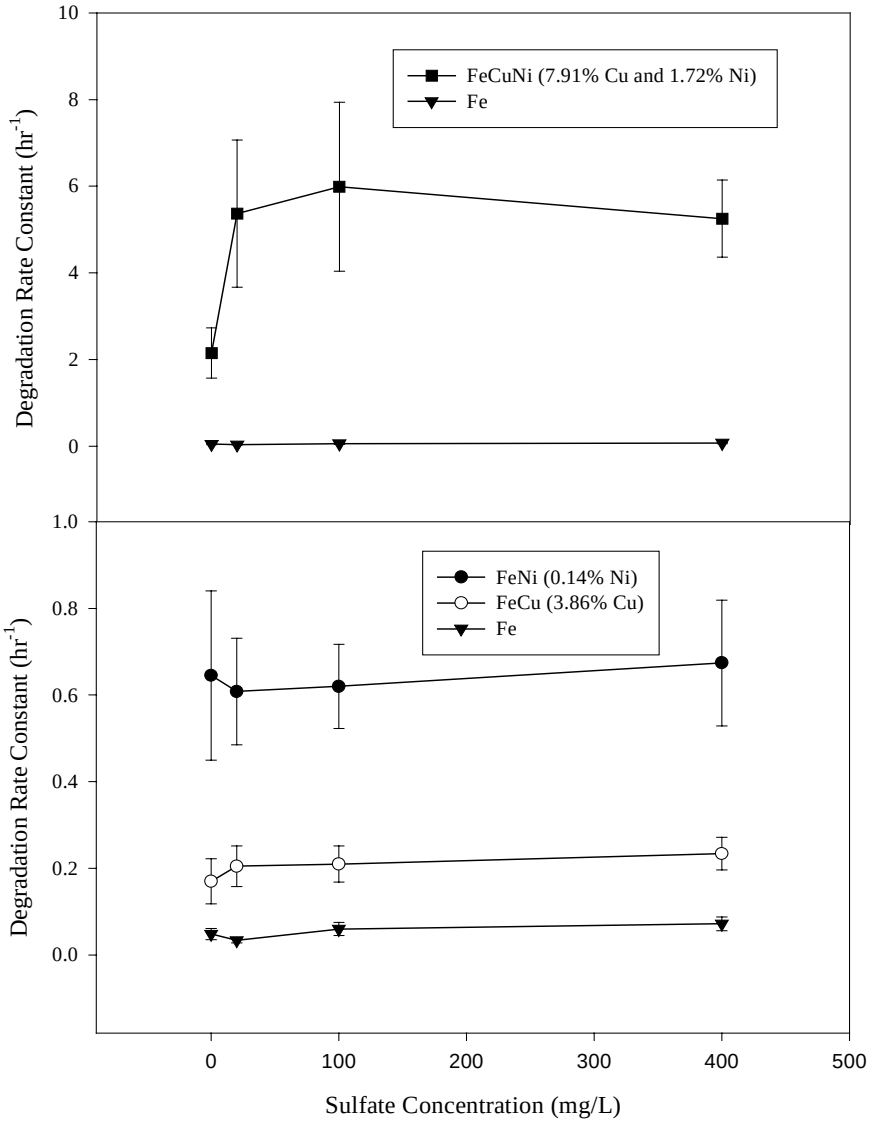

Figure 4.7. SO_4^{2-} Effects on the TCE Degradation Rate Constant
(error bar - 90% confidence interval)

that of de-ionized water. However, if the concentration of HCO_3^- was more than 400 mg/L, HCO_3^- enhanced the degradation rates of TCE at 90% confidence interval as compared to that of de-ionized water.

Effects of SO_4^{2-} on TCE Degradation Rate

For the trimetal Fe/Cu/Ni, the degradation rate of TCE in the SO_4^{2-} solution increased as compared to that that of using de-ionized water. However, at SO_4^{2-} concentrations of 100 mg/L and 400 mg/L, the degradation rates were statistically the same as that for a solution with 20 mg/L SO_4^{2-} (Figure 4.7). For Fe/Ni, Fe/Cu and Fe, SO_4^{2-} solution did not affect the TCE degradation rate at 90% confidence interval. Measurements of SO_4^{2-} concentration indicated that SO_4^{2-} did not change throughout the experiments.

Effects of PO_4^{3-} on the TCE Degradation Rate

For Fe/Cu/Ni, PO_4^{3-} solution slightly enhanced the TCE degradation rates as compared to de-ionized water at 90% confidence level (Figure 4.8). For Fe/Ni, Fe/Cu, and Fe, PO_4^{3-} solution has no effect on the TCE degradation rate at 90% confidence interval. The concentration of PO_4^{3-} did not change throughout the reaction period.

Discussion on Effects of Anions

As presented in Figure 4.5, NO_3^- seemed to have different effects on the degradation rates of TCE using different reductants. When TCE was degraded, NO_3^- was degraded at the same time. For Fe/Cu/Ni, if NO_3^- concentration was less than 20 mg/L, NO_3^- seemed to enhance the degradation rates of TCE at 90% confidence interval as compared to de-ionized water. But if NO_3^- concentration was more than 60 mg/L, NO_3^- may inhibited the degradation rates of TCE. For Fe/Ni, increasing the NO_3^- concentrations from 5 mg/L to 20 mg/L did not significantly affect the degradation rates of TCE. If NO_3^- concentration was or more than 60 mg/L, the degradation rate of TCE was inhibited. Competition between NO_3^- and TCE seemed to have no effect on the degradation of TCE with Fe/Ni, Fe/Cu, and Fe at the range of NO_3^- concentration from 5 mg/L to 60 mg/L. The results were different from those of Senzaki and Kumagai (1988) and Siantar et al. (1996). The studies of Senzaki and Kumagai (1988) indicated that the presence of NO_3^- inhibited the degradation of chlorinated organic compounds. The results of Siantar et al. (1996) similarly showed that NO_3^- decreased the rate of 1,2-Dibromo-3-chloropropane (DBCP) by $\leq$ 50%. A possible reason for the difference is the different ratio of zero-valent iron/volume used. This study used 200 g Fe/L while Siantar et al. (1996) used 36.4 g Fe/L. The larger ratio of zero-valent iron/volume may provide sufficient electrons to degrade both TCE and NO_3^- at the same time. In this situation, the presence of NO_3^- did not affect the degradation of TCE.

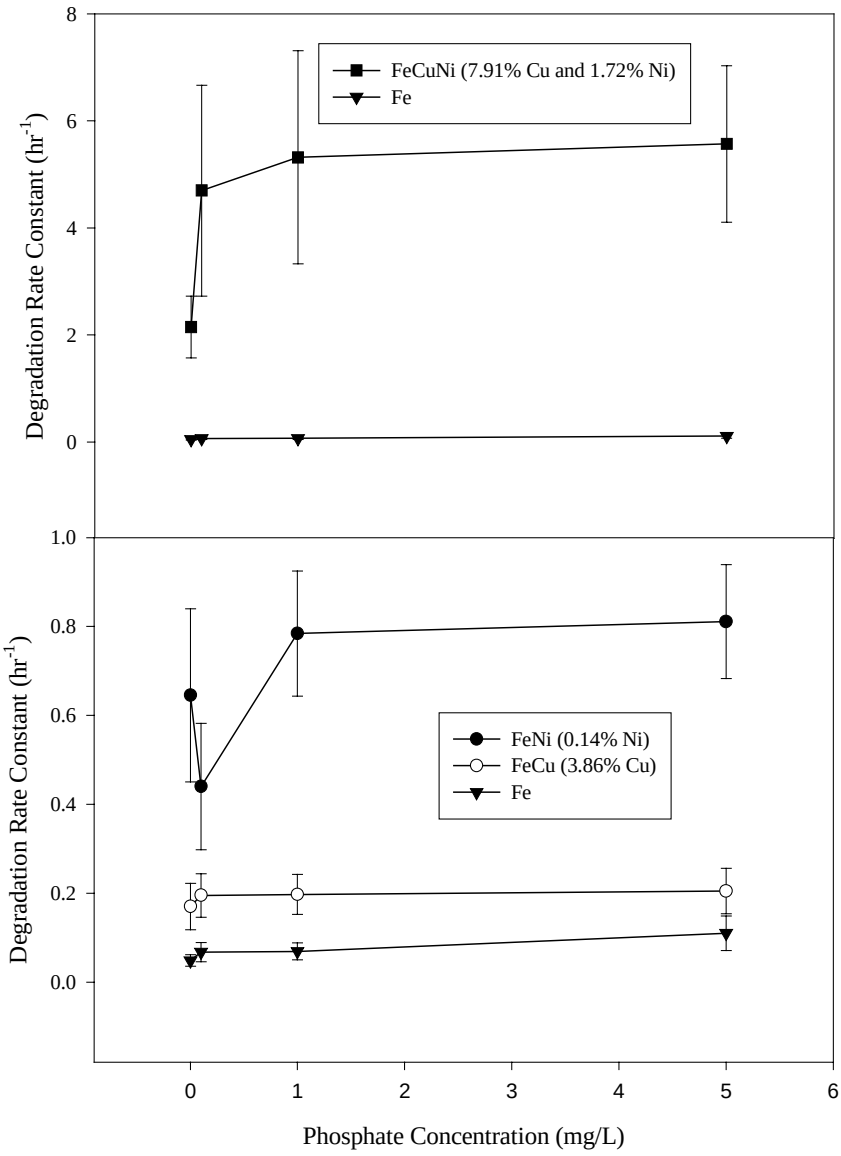

Figure 4.8 PO_4^{3-} Effects on the TCE Degradation Rate Constant
(error bar - 90% confidence interval)

For Fe/Cu/Ni, the degradation rate of TCE in a 5 mg/L and 20 mg/L NO_3^- solution was larger than that of using de-ionized water. The reason for this observation was not clear. As presented earlier, TCE degradation rates at NO_3^- concentrations of 5 mg/L and 20 mg/L were similar. But when the NO_3^- concentration was increased to 60 mg/L, the degradation rate of TCE was decreased. The reduction in degradation rates of TCE may be due to competition. For example using 200 mg/L NO_3^-, 40% of the TCE was degraded after 1.6 hr while 27% of the NO_3^- was removed. Other than the possible competition with NO_3^-, the high concentration of NO_3^- may cause passivation on the surface of Fe/Cu/Ni. In another study by Farrell et al. (2000), They measured the iron corrosion rates in nitrate solution of a 5 mM $Ca(NO_3)_2$ and found that nitrate contributed to increased iron surface passivation and decreased rates of iron corrosion. Competition and passivation may have caused the degradation rate of TCE in the 200 mg/L NO_3^- solution to be much slower than that of using 60 mg/L NO_3^- solution. This study indicated that Fe/Cu/Ni was more sensitive to NO_3^- at a concentration of 200 mg/L than that of Fe/Ni, Fe/Cu, and Fe.

With HCO_3^-, there were no significant effects on the degradation of TCE at HCO_3^- concentrations ranging from 50 mg/L to 800 mg/L for Fe/Cu/Ni, Fe/Ni and Fe/Cu. No precipitation of carbonate was detected by X-ray diffraction. This may be due to the low production of precipitation of carbonate during the short reaction time (2 hr - 2days). A study of the permeable reactive barrier (PRB) at the Denver Federal Center indicated that calcite and siderite precipitation occurred and the porosity of the barrier were reduced by about 0.35% per year (McMahan et al., 1999). The operation of another reactive barriers showed that clogging did not appear to impede groundwater flow and was only occurring in a small area (Vidumsky, 2000). Precipitation of carbonate and phosphate may shorten the life span of the PRBs and increase the cost of PRBs. In addition, the decrease in permeability probably caused channeling resulting in preferential flow through the barrier and escaping the PRB's capture zone (Vidumsky, 2000).

Sulfate had no significant effect on the degradation of TCE using Fe/Ni, Fe/Cu, and Fe but increased the degradation rates of TCE using Fe/Cu/Ni when the sulfate concentration changed from 20 to 400 mg/L. Senzaki and Kumagai (1988) found that SO_4^{2-} increased the degradation rates of 1,1,2,2-tetrachloroethane by electrolytic iron powder as compared to that for de-ionized water. Reduction by green rust may be a reason for the increase in degradation rates of chlorinated organic compounds in the presence of SO_4^{2-}. A study on iron corrosion by Gui and Devine (1994) indicated that in a Na_2SO_4 solution, the sulfate ion was incorporated into the iron hydroxide phase and may be formed as a separate phase known as green rust (Hansen, 1994; Refait and Genin, 1994). Green rust minerals are mixed-valent iron hydroxide minerals consisting of layers of positively charged hydroxide sheets with interlayers containing anions such as chloride, sulfate, and carbonate (Williams and Scherer, 1999). Because green rust is extremely sensitive to oxidation, they are stable only in anoxic environments such as hydromorphic soils (Williams and Scherer, 1999). Precipitation of green rust was easily maintained at a slightly basic pH (Taylor, 1985). X-ray diffraction analysis of the surface at the end of the experiments did not indicate the presence of green rust at the highest concentration of SO_4^{2-} (400 mg/L). It is possible that the amount of green rust produced was too small to be detected by X-ray diffraction. Also, the presence of oxygen which

may be absorbed onto the surface of metal may cause the green rust to be redissolved when the sample was exposed to atmosphere.

Phosphate at concentrations similar to groundwater had no significant effect on the degradation of TCE for Fe/Ni, Fe/Cu, and Fe. This result was different from the study of Senzaki and Kumagai (1988) where they found that PO_4^{3-} increased the degradation rate as compared to that of de-ionized water. But for Fe/Cu/Ni, PO_4^{3-} increased the degradation rate of TCE as compared to that of de-ionized water.

CONCLUSIONS

General Conclusions

In this research, degradation of TCE with bimetals (Fe/Cu and Fe/Ni) and trimetals (Fe/Cu/Ni) and the effects of anions (HCO_3^-, SO_4^{2-}, PO_4^{3-}, and NO_3^-) on the degradation were investigated. The followings are the main conclusions:

1. Two to three percent of C_4H_8 and trace amount of other $C_3 - C_6$ alkenes and alkanes and trace amounts of unidentified byproducts were produced in the experiments for Fe, bimetals and trimetals. The production of partially dechlorinated compounds increased in the sequence of Fe/Cu, Fe/Cu/Ni, Fe/Ni and Fe.

2. The first-order degradation rates for Fe/Cu ranged from 0.15 to 0.64 hr^{-1}. The degradation rate of Fe/Cu reached a maximum for a Cu content of 9.26% which was 10 times higher than the rate with Fe only.

3. The first-order degradation rates for Fe/Ni ranged from 0.66 to 1.90 hr^{-1}. In the case of Fe/Ni, the maximum degradation rate was obtained for a Ni content of 0.25% and was 30 times higher than the rate using Fe only.

4. The first-order degradation rates for Fe/Cu/Ni were from 1.28 to 3.20 hr^{-1}. The maximum degradation rate was obtained for a copper content of 4.17% and a nickel content of 0.40% and was about 50 times higher than that of Fe only.

5. If degradation rates are not considered , reductant Fe/Cu seemed to be better than Fe/Cu/Ni since a lower amount of partially dechlorinated compounds were produced.

6. Addition of Cu and/or Ni to zero-valent iron appeared to increase the degradation of TCE by at least one to two orders of magnitude. Bimetals and trimetals, therefore, can be used as an efficient approach for the degradation of TCE.

7. Competition between NO_3^- and TCE was present but did not affect the degradation rates of TCE with Fe/Ni and Fe/Cu until the concentration of NO_3^- was more than 60 mg/L for Fe/Cu and 20 mg/L for Fe/Ni.

8. Except for an increase in the degradation rate of TCE for 20 mg/L SO_4^{2-} as compared to de-ionized water, SO_4^{2-} did not have an effect on the degradation rates of TCE for Fe/Cu/Ni, Fe/Ni, Fe/Cu, and Fe.

9. For Fe/Cu/Ni, nitrate enhanced the degradation rate of TCE but if concentration of NO_3^- was more than 60 mg/L, NO_3^- inhibited the degradation rate of TCE.

10. Of the four reductants used (Fe/Cu/Ni, Fe/Ni, Fe/Cu and Fe), nitrate had the greatest effect on Fe/Cu/Ni.

11. For Fe/Cu/Ni, an increase in the degradation rate of TCE was observed in SO_4^{2-} or PO_4^{3-} solution as compared to nanopure water, but SO_4^{2-} and PO_4^{3-} did not affect the degradation rates of TCE for Fe/Cu, Fe/Ni and Fe.

12. The presence of HCO_3^- did not affect the rates of TCE dechlorination with Fe/Cu/Ni, Fe/Ni, Fe/Cu, and Fe.

Outstanding Issues

The following are some outstanding issues that need further investigation:

1. The exact pathway for the reductive dechlorination of TCE using copper-plated iron, nickel-plated iron, or copper/nickel-plated iron is still unclear. In addition. the daughter products produced appeared to be different for different bimetals and some were not identified.

2. The reason behind the enhanced degradation of TCE with copper-plated iron, nickel-plated iron, or copper/nickel-plated iron is still unknown.

3. The characteristics of copper or nickel plated on the surface of iron need to be investigated. Knowing the surface properties of these bimetals and trimetals will assist further development and understanding of the mechanism of TCE degradation.

4. The long-term performance of copper-plated iron, nickel-plated iron, or copper/nickel-plated iron needs further research. The effects of different groundwater quality on long-term performance have not been well researched.

Information Transfer Program

Basic Information

Title:	Construction of a soil pit for natural resource education for school children, field day participants and research farm visitors
Start Date:	3/1/2000
End Date:	6/30/2000
Descriptors:	Demonstration, natural resources education
Lead Institute:	Iowa State Water Resources Research Institute
Principal Investigators:	Kenneth T. Pecinovsky

Publication

When giving tours of the soil pit to our targeted audience, such as crop/livestock producers, urban and rural farm visitors and students (kindergarten through high school), we plan to educate and explain the various activities in the pit and relate it to current issues pertaining to water quality in our area. Effects of sinkholes, ag drainage wells, Karst topography, hydrology, commercial nutrient and manure movement (nitrogen and phosphorous), bacteria, and benefits of soil conservation on water quality can be addressed by ISU Cooperative Extension Service and Research Farm personnel. Current related results of research on water quality and hydrology, being conducted on the ISU NE Research and Demonstration Farm can be used to educate visitors and field day participants at the soil pit site also. Another targeted audience, would be the urban, non-farm students and foreign visitors tours at the farm, many of which have probably not seen our natural resources underground, or that can make comparisons to their areas of origin.

USGS Summer Intern Program

Student Support

Student Support					
Category	**Section 104 Base Grant**	**Section 104 RCGP Award**	**NIWR-USGS Internship**	**Supplemental Awards**	**Total**
Undergraduate	1	0	0	0	1
Masters	4	2	0	0	6
Ph.D.	1	0	0	0	1
Post-Doc.	3	0	0	0	3
Total	9	2	0	0	11

Notable Awards and Achievements

This year we have tried to increase our visibility in the state in a number of ways.

We have initiated a Water Resources Seminar Series that brought in key personnel from across the state and abroad who have interest in water resources.

We have initiated an awards program to honor Iowa citizens for their contributions to water resources. Awards were presented in the following five categories: Outstanding Undergraduate Student; Outstanding Graduate Student; Outstanding Educator; Outstanding Researcher; and Outstanding Citizen. The awards were presented at the "Agriculture and The Environment: State and Federal Water Initiatives" conference which was held in March and was co-sponsored by ISWRRI.

ISWRRI was also involved in another conference, "The Kirkham Conference" which honored Professor Don Kirkham, who, among other things, was the first Director of the Iowa State Water Resources Research Institute.

We have also begun a summer internship program. This year we have seven interns who will be working from 8-10 weeks at universities, state agencies, and the USGS.

This year we are initiating a semi-annual newsletter and continue to update our website.

Publications from Prior Projects

None